The EMBO Journal (2012) 31, 4258–4275 | © 2012 European Molecular Biology Organization | All Rights Reserved 0261-4189/12
www.embojournal.org

THE EMBO JOURNAL

Arginine methylation next to the PY-NLS modulates Transportin binding and nuclear import of FUS

Dorothee Dormann[1,*], Tobias Madl[2,3,4,13], Chiara F Valori[5,6,13], Eva Bentmann[1], Sabina Tahirovic[7], Claudia Abou-Ajram[1], Elisabeth Kremmer[8], Olaf Ansorge[9], Ian RA Mackenzie[10], Manuela Neumann[5,6,11] and Christian Haass[1,7,12,*]

[1]Adolf-Butenandt-Institute, Biochemistry, Ludwig-Maximilians-University, Munich, Germany, [2]NMR Spectroscopy, Karl-Franzens University, Graz, Austria, [3]Institute of Structural Biology, Helmholtz Zentrum München, Neuherberg, Germany, [4]Biomolecular NMR, Department of Chemistry, Technische Universität München, Garching, Germany, [5]Institute of Neuropathology, University Hospital Zurich, Zurich, Switzerland, [6]DZNE—German Center for Neurodegenerative Diseases, Tübingen, Germany, [7]DZNE—German Center for Neurodegenerative Diseases, Munich, Germany, [8]Institute of Molecular Immunology, Helmholtz Zentrum München, Munich, Germany, [9]Department of Neuropathology, John Radcliffe Hospital, Oxford, UK, [10]Department of Pathology, Vancouver General Hospital, Vancouver, Canada, [11]Department of Neuropathology, University of Tübingen, Tübingen, Germany and [12]Munich Cluster for Systems Neurology (SyNergy), Munich, Germany

Fused in sarcoma (FUS) is a nuclear protein that carries a proline-tyrosine nuclear localization signal (PY-NLS) and is imported into the nucleus via Transportin (TRN). Defects in nuclear import of FUS have been implicated in neurodegeneration, since mutations in the PY-NLS of FUS cause amyotrophic lateral sclerosis (ALS). Moreover, FUS is deposited in the cytosol in a subset of frontotemporal lobar degeneration (FTLD) patients. Here, we show that arginine methylation modulates nuclear import of FUS via a novel TRN-binding epitope. Chemical or genetic inhibition of arginine methylation restores TRN-mediated nuclear import of ALS-associated FUS mutants. The unmethylated arginine–glycine–glycine domain preceding the PY-NLS interacts with TRN and arginine methylation in this domain reduces TRN binding. Inclusions in ALS-FUS patients contain methylated FUS, while inclusions in FTLD-FUS patients are not methylated. Together with recent findings that FUS co-aggregates with two related proteins of the FET family and TRN in FTLD-FUS but not in ALS-FUS, our study provides evidence that these two diseases may be initiated by distinct pathomechanisms and implicates alterations in arginine methylation in pathogenesis.

*Corresponding authors. D Dormann or C Haass, Adolf-Butenandt-Institute, Biochemistry, Ludwig-Maximilians-University, DZNE—German Center for Neurodegenerative Diseases, Schillerstr 44, Munich 80336, Germany. Tel.: +49 89 218075474; Fax: +49 89 218075415; E-mail: dorothee.dormann@dzne.lmu.de or Tel.: +49 89 218075471; Fax: +49 89 218075415; E-mail: christian.haass@dzne.lmu.de
[13]These two authors contributed equally to this work

Received: 26 March 2012; accepted: 17 August 2012; published online: 11 September 2012

The EMBO Journal (2012) **31,** 4258–4275. doi:10.1038/emboj.2012.261; Published online 11 September 2012
Subject Categories: neuroscience
Keywords: amyotrophic lateral sclerosis (ALS); arginine methylation; frontotemporal lobar degeneration (FTLD); fused in sarcoma (FUS); Transportin (TRN)

Introduction

Fused in sarcoma (FUS), also known as translocated in liposarcoma (TLS), is a nucleic acid-binding protein that is predominantly localized in the nucleus and has been implicated in various nuclear processes, such as transcription, splicing and microRNA processing (Lagier-Tourenne *et al*, 2010). Recently, mutations in *FUS* have been described as a cause of familial amyotrophic lateral sclerosis (ALS) (Kwiatkowski *et al*, 2009; Vance *et al*, 2009). ALS is an incurable adult-onset neurodegenerative disease of the human motor system. It is characterized by motor neuron degeneration in the brainstem and spinal cord, leading to progressive paralysis and eventually death due to respiratory muscle failure, typically within 1–5 years of disease onset (Kiernan *et al*, 2011). The majority of ALS cases are sporadic, but about 10% are inherited in a dominant manner (familial ALS, fALS) (Da Cruz and Cleveland, 2011). Of these, about 4% are caused by mutations in the *FUS* gene on chromosome 16 (ALS-FUS). Most pathogenic mutations identified so far are located at the very C-terminus of the FUS protein and affect a proline-tyrosine nuclear localization signal (PY-NLS) (Lee *et al*, 2006) (Figure 1A). This non-classical NLS is bound by the nuclear import receptor Transportin (TRN), also known as Karyopherin β2 (Kapβ2), which translocates PY-NLS-containing cargo proteins across the nuclear pore complex (Chook and Suel, 2011). Pathogenic *FUS* mutations affect key residues of the PY-NLS or completely delete the signal sequence and thus impair nuclear import of FUS (Bosco *et al*, 2010; Dormann *et al*, 2010; Kino *et al*, 2010; Gal *et al*, 2011; Ito *et al*, 2011; Zhang and Chook, 2012). This nuclear transport defect is directly involved in pathogenesis, since mutations that cause a very severe nuclear import block (e.g., FUS-P525L) cause an unusually early disease onset and rapid disease course (Chio *et al*, 2009; Baumer *et al*, 2010; Bosco *et al*, 2010; DeJesus-Hernandez *et al*, 2010; Dormann *et al*, 2010; Waibel *et al*, 2010; Yan *et al*, 2010). Moreover, the FUS protein is deposited in abnormal protein inclusions in neurons and glia of ALS-FUS patients and nuclei often show a reduced FUS staining (Kwiatkowski *et al*, 2009; Vance *et al*, 2009; Blair *et al*, 2010; Groen *et al*, 2010; Hewitt *et al*, 2010; Rademakers *et al*, 2010; Mackenzie *et al*, 2011), further supporting the idea that nuclear import of FUS might be disturbed in this disease.

After the discovery of *FUS* mutations in familial ALS, FUS was studied in a related neurodegenerative disorder, frontotemporal lobar degeneration (FTLD), since ALS and FTLD share many clinical and pathological features (Lomen-Hoerth *et al*, 2002; Murphy *et al*, 2007; Mackenzie *et al*, 2010b). This revealed that FUS is also a component of the abnormal protein inclusions in several subtypes of FTLD, subsequently termed FTLD-FUS (Mackenzie *et al*, 2010a). In contrast to ALS-FUS, which is caused by *FUS* mutations, no genetic alterations in the *FUS* gene have so far been identified in FTLD-FUS cases (Neumann *et al*, 2009a, b; Urwin *et al*, 2010; Snowden *et al*, 2011). Thus, the pathological redistribution of FUS in these cases cannot be explained by a mutant PY-NLS, suggesting that a more general dysregulation of TRN-mediated transport may underlie FUS pathology and neurodegeneration in FTLD-FUS. This is supported by the recent finding that in addition to FUS, two related PY-NLS-containing proteins, Ewing sarcoma protein (EWS) and TATA-binding protein-associated factor 15 (TAF15), which belong to the same protein family (FET family), as well as TRN, are present in inclusions of FTLD-FUS patients (Brelstaff *et al*, 2011; Neumann *et al*, 2011, 2012; Davidson *et al*, 2012). How this pathological redistribution and co-deposition of FUS, EWS and TAF15 and TRN occurs in FTLD-FUS is currently unknown.

Nucleocytoplasmic transport can be regulated at multiple levels, including post-translational modifications of transport cargo, such as phosphorylation or ubiquitination (Terry *et al*, 2007). In addition, arginine methylation, which is a common post-translational modification of nuclear RNA-binding proteins, has been described to affect nuclear localization of several proteins, although the regulatory mechanism(s) are still largely unknown (Bedford and Clarke, 2009). Arginine methylation involves transfer a methyl group from *S*-adenosyl-L-methionine (SAM) onto one or both of the guanidinium nitrogens of the arginine side chain with the help of protein *N*-arginine methyltransferases (PRMTs), resulting in monomethylarginine, symmetric or asymmetric dimethylarginine residues (Pahlich *et al*, 2006). This alters the hydrophobicity and hydrogen bonding capacity of the modified arginine residues and can affect protein–protein interactions (Bedford and Clarke, 2009; Pahlich *et al*, 2006). FUS, EWS and TAF15 have been described to undergo extensive asymmetric dimethylation in their arginine–glycine–glycine (RGG) domains (Figure 1A) (Belyanskaya *et al*, 2001; Lee and Bedford, 2002; Rappsilber *et al*, 2003; Ong *et al*, 2004; Araya *et al*, 2005; Pahlich *et al*, 2005; Hung *et al*, 2009; Jobert *et al*, 2009; Du *et al*, 2011), and there is evidence that arginine methylation can affect their nucleocytoplasmic localization (Araya *et al*, 2005; Jobert *et al*, 2009; Tradewell *et al*, 2012). However, the molecular mechanism by which arginine methylation may affect nuclear localization of the FET proteins is unknown and it is unclear whether arginine methylation is involved in the pathology of ALS/FTLD-FUS.

We now show that arginine methylation impairs TRN-dependent nuclear import of FUS, by decreasing binding of TRN to a novel TRN-binding motif next to the PY-NLS of FUS. Furthermore, immunohistochemistry with novel methyl-FUS-specific antibodies revealed that inclusions in ALS-FUS patients contain methylated FUS, while deposited FUS in FTLD-FUS cases is unmethylated. Our findings provide new insights into the mechanism of TRN-cargo recognition in general and suggest that altered arginine methylation of FET proteins may be involved in the pathological co-deposition of FET proteins and TRN in FTLD-FUS.

Results

Inhibition of methylation restores nuclear localization of ALS-associated FUS mutants

To test if arginine methylation affects the nuclear localization of FUS, we treated HeLa cells with the general methylation inhibitor, adenosine-2,3-dialdehyde (AdOx), which inhibits all SAM-dependent enzymatic reactions, including protein arginine methylation (Chen *et al*, 2004), and analysed its effect on localization of HA-tagged wild-type FUS (WT) and four cytoplasmically mislocalized ALS-associated FUS mutants (Dormann *et al*, 2010). Consistent with our previous findings, FUS-WT was located almost exclusively in the nucleus in untreated cells, whereas the ALS-associated FUS mutants showed a varying degree of cytoplasmic mislocalization, ranging from a very mild mislocalization for R521G, over an intermediate phenotype for R524S and R522G, to a severe mislocalization for P525L (Figure 1B upper panels, see C for quantification). Strikingly, upon treatment of cells with AdOx, all FUS mutants showed a predominant nuclear localization and were almost indistinguishable from the WT protein (Figure 1B lower panels and C). This could not be attributed to altered expression levels, since similar HA–FUS protein levels were observed in untreated and AdOx-treated cells (Figure 1D). Thus, inhibition of methylation with AdOx restores nuclear localization of ALS-associated FUS mutants, suggesting that nuclear import of FUS might be modulated by arginine methylation.

The same phenomenon could also be observed in primary rat hippocampal neurons, where FUS-WT was located almost exclusively in the nucleus (0% cells with mislocalized FUS), while the P525L mutant was partially mislocalized to the cytosol, including neuritic processes, in the majority of neurons ($89 \pm 1\%$) (Figure 1E). AdOx treatment significantly reduced the cytoplasmic mislocalization of FUS-P525L ($26 \pm 12\%$ cells with mislocalized FUS, $P < 0.05$). Thus, nuclear localization of mutant FUS is affected by methylation not only in transformed cell lines, but also in primary neurons, demonstrating that this is not a cell-type-specific phenomenon.

Methylation affects nuclear localization of FET protein mutants

Since not only FUS but also the other FET family members, EWS and TAF15, are subject to arginine methylation (Belyanskaya *et al*, 2001; Ong *et al*, 2004; Araya *et al*, 2005; Pahlich *et al*, 2005; Jobert *et al*, 2009) and the three proteins share a very similar domain structure (Figure 2A), we speculated that arginine methylation may regulate nuclear import of all FET proteins in a similar manner and may contribute to their pathological deposition in FTLD-FUS (Neumann *et al*, 2011; Davidson *et al*, 2012). To test this hypothesis, we mutated the PY-NLS of EWS (EWS-P655L) and TAF15 (TAF-P591L) to generate cytoplasmic point mutants analogous to FUS-P525L. In contrast to WT EWS and TAF15, EWS-P655L and TAF-P591L were partially mislocalized to the cytoplasm (Figure 2B, see C for quantification). Upon treatment with

AdOx, all three FET protein mutants became predominantly nuclear, suggesting that nuclear localization of all FET family members is affected by methylation in a similar manner.

Silencing of protein N-arginine methyltransferase 1 (PRMT1) causes nuclear localization of FUS-P525L

AdOx inhibits all SAM-dependent pathways including DNA, lipid and protein methylation (Bartel and Borchardt, 1984; Liteplo and Kerbel, 1986). Therefore, the above-described relocalization of FUS mutants by AdOx could depend on any of these mechanisms. FUS has been previously reported to be asymmetrically dimethylated on arginine residues (Rappsilber *et al*, 2003; Ong *et al*, 2004) and it is known that protein arginine methylation can affect subcellular localization of various proteins (reviewed in Bedford and Clarke, 2009). We therefore speculated that

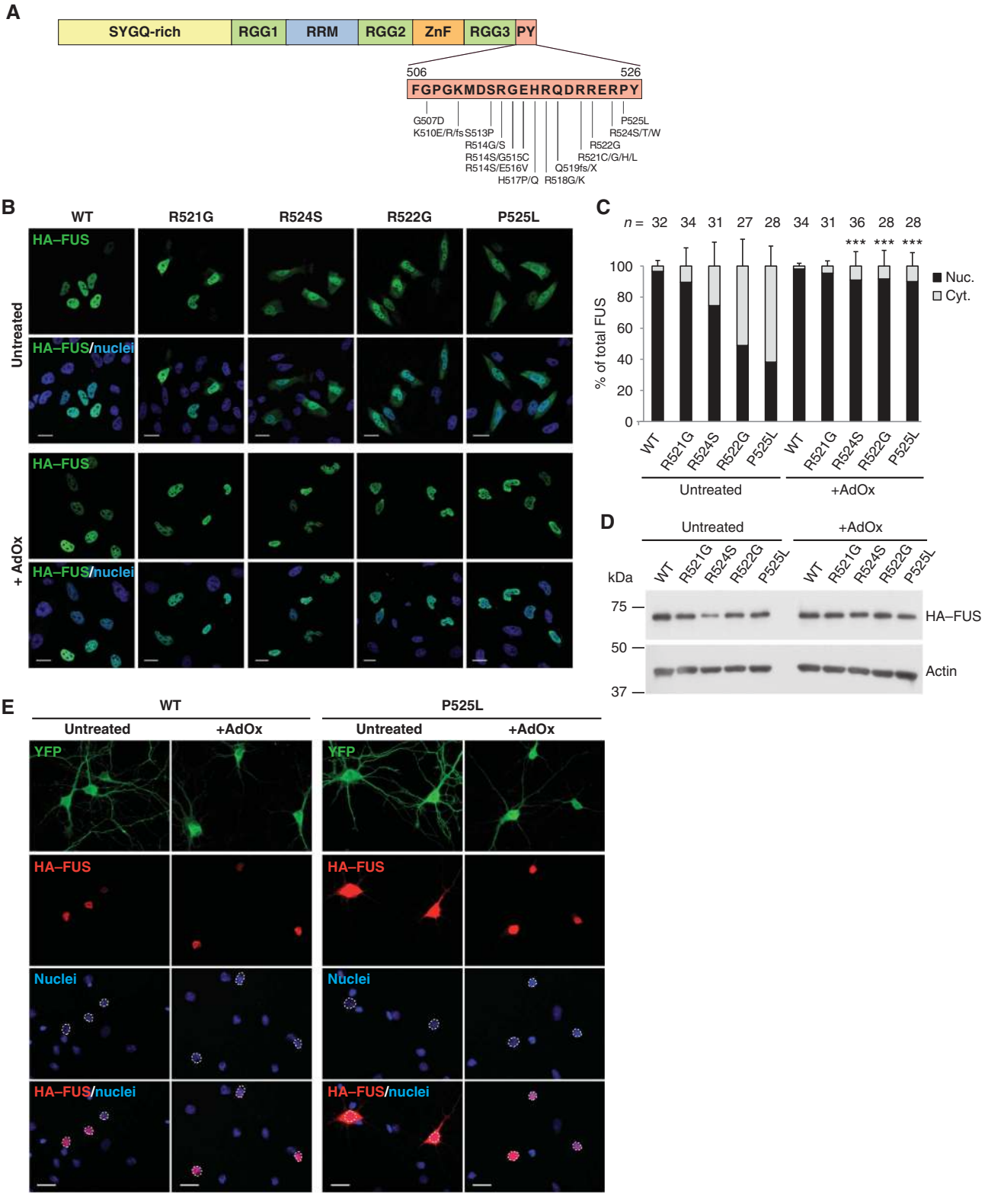

specifically inhibition of arginine methylation could be responsible for the striking relocalization of FUS mutants upon AdOx treatment.

To test this hypothesis, we silenced the major protein arginine methyltransferase predominantly responsible for most asymmetric arginine dimethylation, protein *N*-arginine methyltrasferase 1 (PRMT1) (Pawlak *et al*, 2000; Tang *et al*, 2000), using two different PRMT1-specific siRNAs. Two days after siRNA delivery, HA-tagged FUS-WT or FUS-P525L was transfected into cells and their localization was examined by confocal microscopy. Consistent with our hypothesis, silencing of PRMT1 caused a predominantly nuclear localization of FUS-P525L, whereas the typical partially cytoplasmic localization could be observed in control siRNA-transfected cells (Figure 3A and B). Rescue of nuclear localization of FUS-P525L, although significant ($P<0.001$), was not as efficient as with AdOx treatment, which could be due to residual amounts of PRMT1 in PRMT1 siRNA-transfected cells (see immunoblot in Figure 3A) or to the methylation of FUS by other PRMTs. Nevertheless, siRNA-mediated silencing of PRMT1 mimicked the effect of AdOx treatment, demonstrating that nuclear localization of mutant FUS is modulated by PRMT1-dependent arginine methylation.

Nuclear import of mutant FUS upon AdOx treatment is Transportin dependent

Nuclear import of FUS has been shown to be mediated by the nuclear import receptor TRN. To test if nuclear localization of FUS-P525L upon AdOx treatment or PRMT1 knockdown is still dependent on TRN, we utilized a TRN-specific inhibitor peptide (M9M), which binds to TRN with high affinity and thus efficiently competes with nuclear import of regular TRN substrates (Cansizoglu *et al*, 2007). In addition, we utilized a similar high-affinity peptide inhibitor (Bimax) for the classical nuclear import receptor Importin α (Kosugi *et al*, 2008), since it is also conceivable that arginine methylation masks a so far unidentified NLS, which would become accessible to Importin α upon methylation inhibition.

We expressed these competitor peptides as GFP fusion proteins (GFP–M9M and GFP–Bimax) together with HA-tagged FUS-P525L in HeLa cells and analysed cellular localization of mutant FUS upon AdOx or mock treatment.

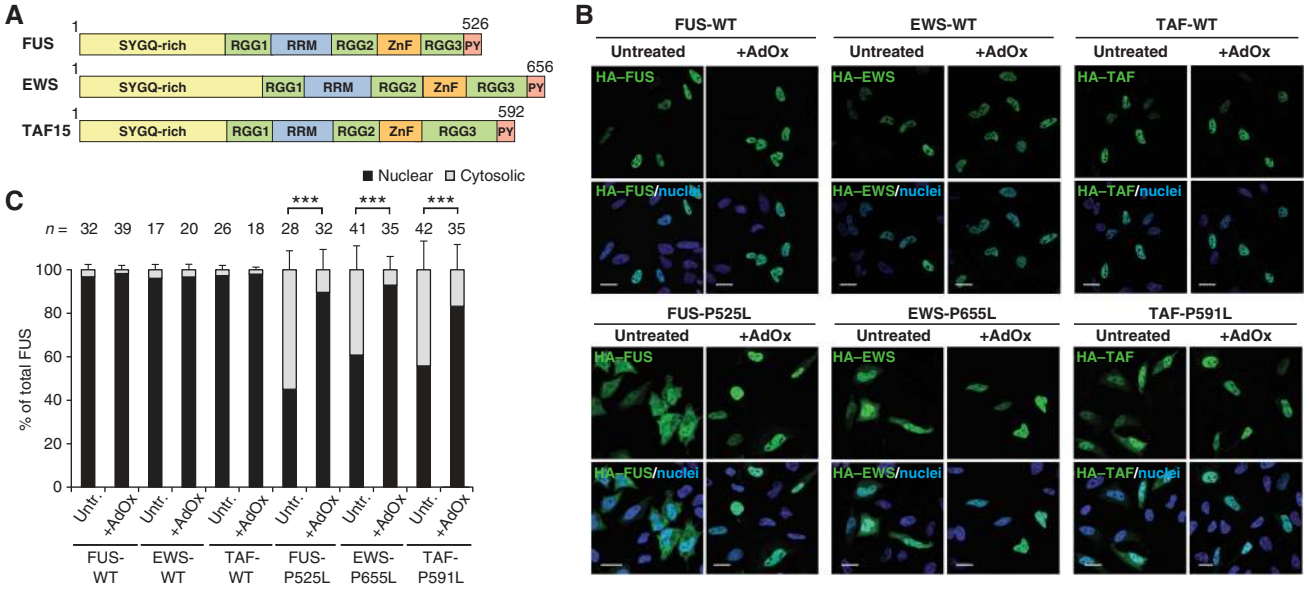

Figure 2 Methylation affects nuclear localization of EWS and TAF15 mutants. (**A**) Schematic diagram showing the domain structures of FUS, EWS and TAF15 (FET proteins). (**B**) Localization of HA-tagged FUS, EWS or TAF15 (WT or with mutant PY-NLS) in untreated or AdOx-treated HeLa cells. Cytoplasmic FET protein mutants become predominantly nuclear upon AdOx treatment, suggesting that methylation affects nuclear import of all FET family members in a similar fashion. Scale bars: 20 μm. (**C**) Quantification of nuclear and cytosolic fluorescence intensities. Values are means across *n* cells, error bars indicate s.d. Statistical significance is displayed as *** ($P<0.001$) (one-way ANOVA).

Figure 1 Cytoplasmic mislocalization of ALS-associated FUS mutants is abrogated upon inhibition of methylation. (**A**) Schematic diagram showing the domain structure of FUS. Sequence of the C-terminal PY-NLS and ALS-causing point mutations within the NLS are given below. ALS-associated mutations outside the PY-NLS are described elsewhere (Mackenzie *et al*, 2010b). SYGQ-rich = serine, tyrosine, glycine, glutamine-rich domain; RRM = RNA recognition motif; ZnF = zinc finger. (**B**) Localization of HA-tagged FUS WT or the indicated ALS-associated FUS mutants in untreated (upper panels) or AdOx-treated (lower panels) HeLa cells. ALS-associated FUS mutants become predominantly nuclear upon AdOx treatment, suggesting that methylation modulates nuclear import of FUS. Scale bars: 20 μm. (**C**) Quantification of nuclear and cytosolic fluorescence intensities. Values are means across *n* cells, error bars indicate standard deviations (s.d.). Statistical significance between untreated and AdOx-treated is displayed as *** ($P<0.001$; one-way ANOVA). (**D**) HA–FUS protein levels in untreated and AdOx-treated HeLa cells were analysed by immunoblotting with an HA-specific antibody (upper panel). Actin served as a loading control (lower panel). AdOx treatment does not affect expression of HA–FUS constructs. (**E**) Localization of HA-tagged FUS-WT or P525L (red) in untreated or AdOx-treated primary rat hippocampal neurons. YFP (green) served as a cytosolic filler protein to visualize neuronal morphology, nuclei were visualized with DAPI. In contrast to untreated neurons, AdOx-treated neurons rarely show cytoplasmic mislocalization of FUS-P525L. Scale bars: 20 μm. Figure source data can be found with the Supplementary data.

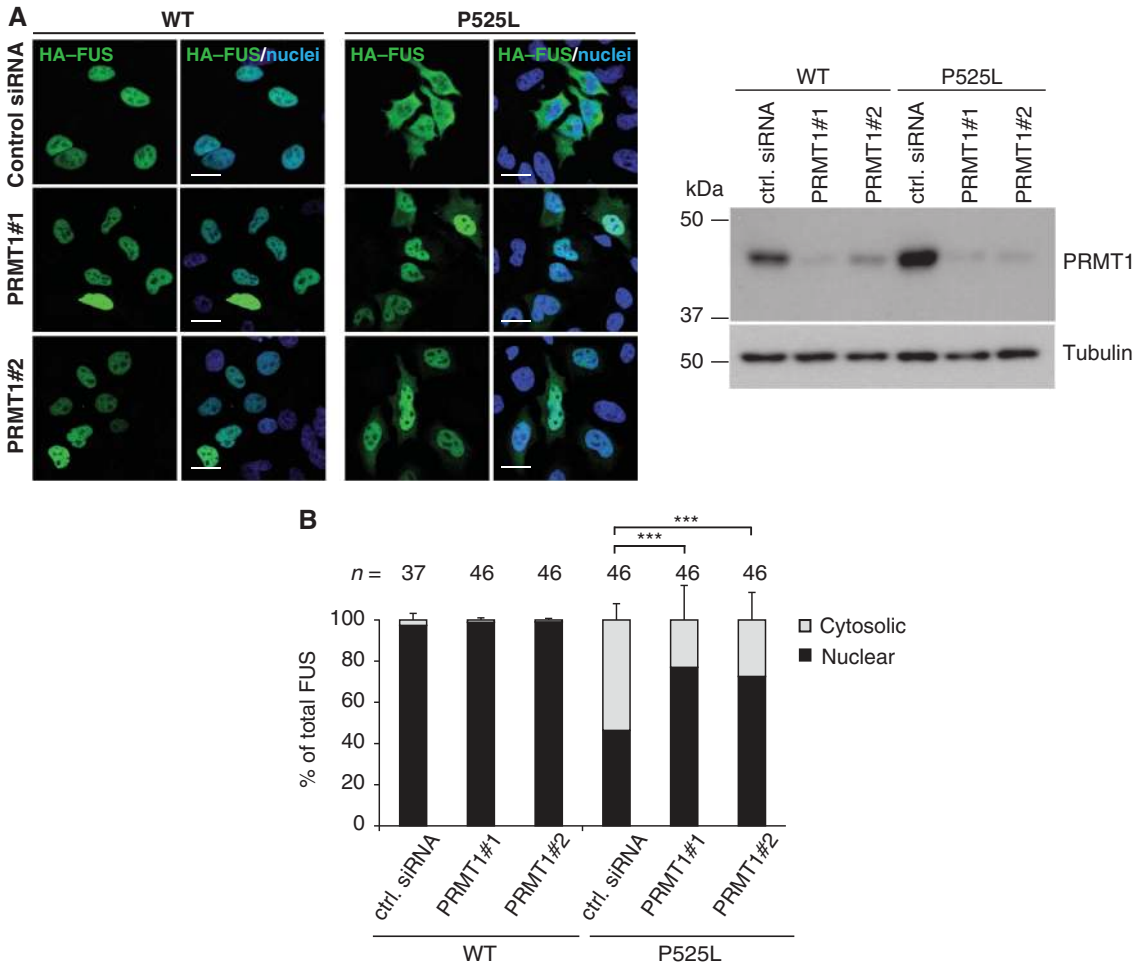

Figure 3 PRMT1 silencing causes increased nuclear localization of FUS-P525L. (**A**) Protein N-arginine methyltransferase 1 (PRMT1) expression was silenced in HeLa cells by transfection of two different siRNAs (PRMT1#1 and PRMT1#2), a control (ctrl.) siRNA was used as a negative control. In all, 48 h after siRNA delivery, cells were transfected with HA-tagged FUS-WT or P525L and localization of these proteins was examined by HA immunostaining (green) and confocal microscopy. PRMT1 knockdown causes a predominantly nuclear localization of the FUS-P525L mutant, suggesting that arginine methylation by PRMT1 modulates nuclear import of FUS. Scale bars: 20 μm. Immunoblots on the right show PRMT1 knockdown efficiency. Total cell lysates were examined with a PRMT1-specific antibody (upper panel) and a tubulin-specific antibody (lower panel). (**B**) Quantification of nuclear and cytosolic fluorescence intensities. Values are means across *n* cells, error bars indicate s.d. Statistical significance is displayed as *** ($P<0.001$) (one-way ANOVA). Figure source data can be found with the Supplementary data.

As expected, in control (GFP)-transfected cells, FUS-P525L showed the above described nuclear localization upon AdOx treatment (Figure 4A, left panels). Consistent with our previous data (Dormann *et al*, 2010), GFP–M9M expression led to recruitment of FUS-P525L into cytosolic stress granules in about half of the cells (Figure 4A, middle panels). However, both in cells with and without stress granules, nuclear accumulation of FUS-P525L upon AdOx treatment was blocked by GFP–M9M expression, demonstrating that TRN activity is required for nuclear import of mutant FUS. In contrast, the classical Importin α-dependent nuclear import pathway does not seem to be involved, since AdOx-mediated nuclear import of FUS-P525L still occurred in cells transfected with the Importin α inhibitor (GFP–Bimax) (Figure 4A, right panels). Thus, nuclear localization of mutant FUS upon AdOx treatment is dependent on TRN, but not Importin α activity.

To investigate whether TRN mediates the above-described relocalization by direct binding of mutant FUS or indirectly via another TRN substrate, we analysed a FUS deletion mutant lacking the most essential amino acids of the FUS PY-NLS (Δ514–526, see schematic diagram in Figure 4B) (Dormann *et al*, 2010; Zhang and Chook, 2012). In contrast to FUS-P525L, which was mostly nuclear upon AdOx treatment, the C-terminal deletion mutant was strongly mislocalized to the cytosol in both untreated and AdOx-treated cells (Figure 4B). This demonstrates that the mutant PY-NLS of FUS is required for nuclear relocalization upon AdOx treatment, suggesting that TRN directly binds to and imports mutant FUS upon inhibition of methylation.

Arginines in the RGG3 domain of FUS are required for nuclear import of mutant FUS

Next, we searched for the mechanism how arginine methylation may regulate TRN-dependent nuclear import of FUS. One possibility would be that, similar to the nuclear poly(A)-binding protein (PABPN1) (Fronz *et al*, 2011), arginine methylation within the PY-NLS of FUS (on residues R514, R518, R521, R522 and/or R524) may affect TRN binding.

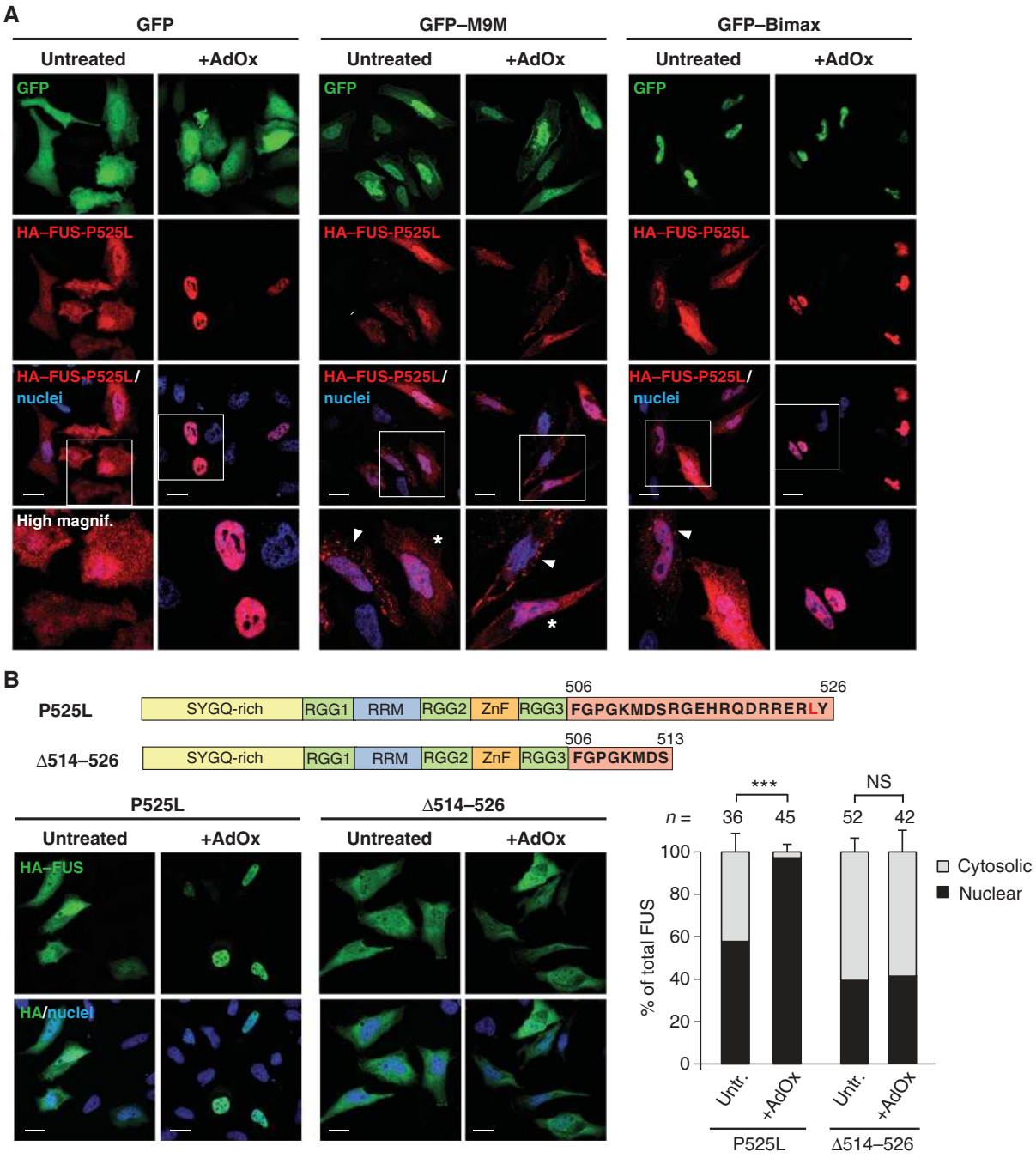

Figure 4 Nuclear import of FUS-P525L upon AdOx treatment is dependent on TRN. (**A**) Localization of HA–FUS-P525L in untreated or AdOx-treated HeLa cells after co-expression of GFP as a control, a competitor of the TRN pathway (GFP–M9M) or a competitor of the Importin α pathway (GFP–Bimax) (green). After HA immunostaining (red), localization of mutant FUS was examined by confocal microscopy. The bottom row shows a higher magnification of the boxed regions. GFP–M9M expressing cells with stress granules are labelled with an arrowhead, cells without stress granules are labelled with an asterisk. Both in cells with and without stress granules, GFP–M9M prevents nuclear import of FUS-P525L upon AdOx treatment, demonstrating that import of FUS-P525L is TRN dependent. Scale bars: 20 μm. (**B**) Localization of a FUS deletion mutant lacking the core amino acids of the C-terminal PY-NLS (Δ514–526, see schematic diagram) in untreated or AdOx-treated HeLa cells. Nuclear relocalization upon AdOx treatment requires the FUS PY-NLS, suggesting that it requires direct TRN binding. Scale bars: 20 μm. Quantification shows nuclear and cytosolic fluorescence intensities. Values are means across *n* cells, error bars indicate s.d. Statistical significance is displayed as *** ($P<0.001$) (one-way ANOVA); NS = not significant.

Another possibility would be that the RGG motifs N-terminal of the PY-NLS could be involved in modulating TRN binding and nuclear import of FUS. The latter scenario would be consistent with the fact that methylated arginines have been exclusively identified in the RGG domains and not the PY-NLS of FUS (Rappsilber *et al*, 2003; Ong *et al*, 2004).

To find out if arginine residues in the PY-NLS or the RGG3 domain mediate the differential localization of mutant FUS upon methylation inhibition, we attached the mutant PY-NLS ($514–526_{P525L}$) alone or with the RGG3 domain ($455–526_{P525L}$) to the C-terminus of the cytosolic reporter protein GST–GFP (see Figure 5A for a schematic diagram). As shown

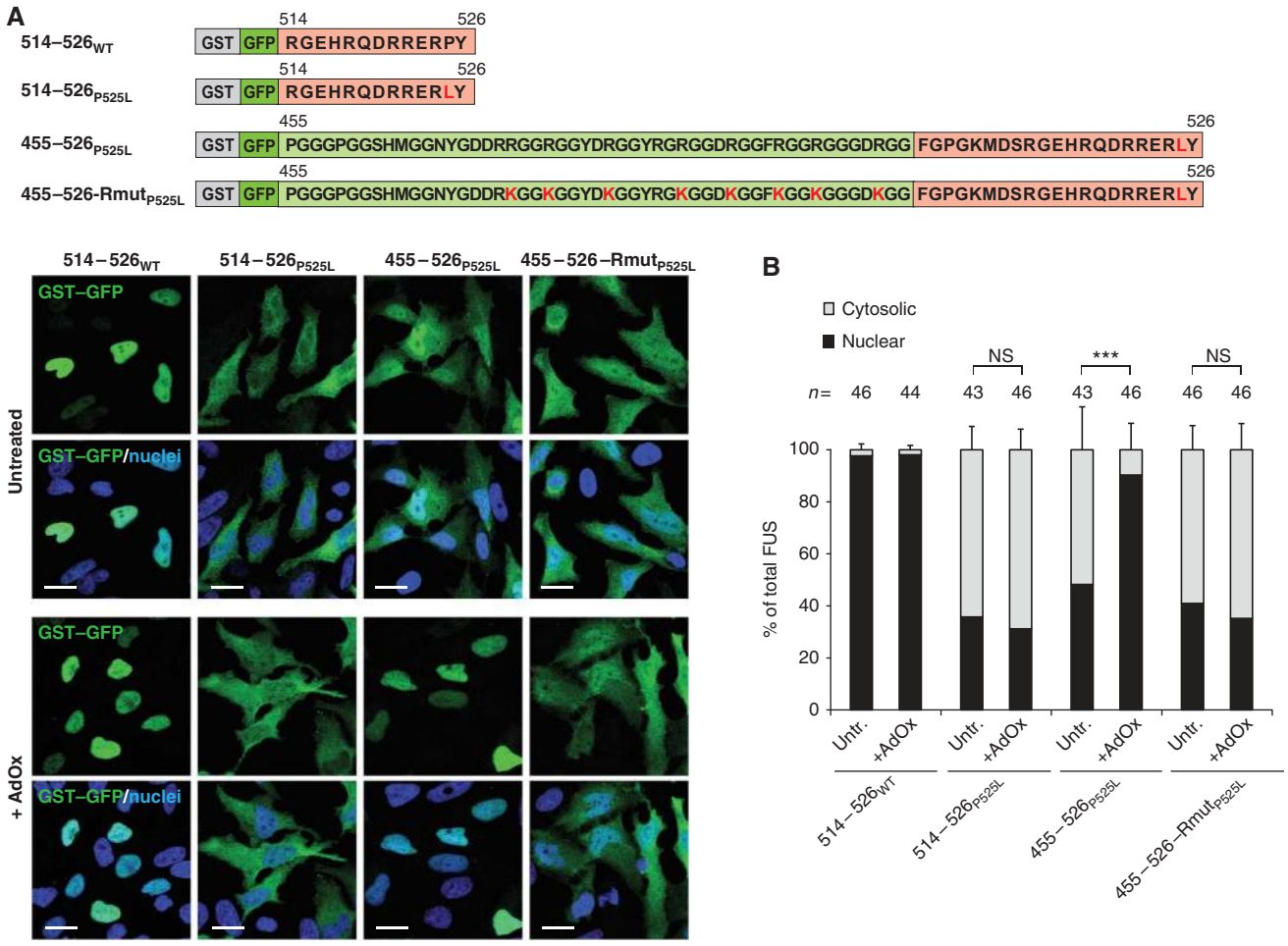

Figure 5 Arginine residues in the RGG3 domain of FUS are required for nuclear import of mutant FUS. (**A**) GST–GFP reporter proteins with the indicated FUS sequences at the C-terminus were transiently expressed in untreated or AdOx-treated HeLa cells. Localization of reporter constructs was examined after GFP (green) immunostaining by confocal microscopy. Arginine residues in the PY-NLS (amino acids 514–526) are not sufficient for restoring nuclear import of the mutant reporter protein upon AdOx treatment, while arginines in the RGG3 domain (amino acids 455–505) are necessary and sufficient for this effect. Scale bars: 20 μm. (**B**) Quantification shows nuclear and cytosolic fluorescence intensities. Values are means across *n* cells, error bars indicate s.d. Statistical significance is displayed as *** ($P<0.001$) (one-way ANOVA); NS = not significant.

previously (Dormann *et al*, 2010), GST–GFP carrying the intact PY-NLS (514–526$_{WT}$) was efficiently imported into the nucleus, while a reporter protein carrying the mutant PY-NLS (514–526$_{P525L}$) failed to be imported efficiently (Figure 5A, see B for quantification). Upon AdOx treatment, the GST–GFP–514–526$_{P525L}$ reporter protein remained predominantly cytoplasmic, demonstrating that the five arginines within the PY-NLS do not mediate nuclear import upon AdOx treatment. In contrast, the reporter protein encompassing the RGG3 domain plus the PY-NLS (455–526$_{P525L}$) fully recapitulated the AdOx-mediated nuclear localization phenotype observed for the full-length protein (Figure 5A and B). A mutant version of this reporter construct, where all arginines within RGG motifs where replaced by lysines (455–526-Rmut$_{P525L}$, see schematic diagram in Figure 5A) and therefore cannot be methylated by PRMT1 (Butler *et al*, 2011), failed to localize to the nucleus upon AdOx treatment. Thus, arginines within the RGG3 domain are necessary and sufficient for restoring nuclear import of the mutant reporter protein upon methylation inhibition.

The RGG3 domain of FUS interacts tightly with TRN and rescues weaker binding of the mutant PY-NLS

To prove that the RGG repeats in the RGG3 domain of FUS directly bind to TRN, we analysed the interaction of recombinant FUS comprising residues 454–526 (FUS454–526$_{WT}$ and FUS454–526$_{P525L}$, see Figure 6A for a schematic diagram) with recombinant TRN by NMR spectroscopy. NMR spectra of FUS454–526$_{WT}$ and FUS454–526$_{P525L}$ in isolation showed that the two proteins are intrinsically disordered, given the distribution of signals in regions characteristic for random coil proteins (Figure 6B). Lack of stable tertiary and secondary structure is a common feature of known PY-NLSs and allows for highly specific binding of a great variety of different transportin cargo proteins (Chook and Suel, 2011). Upon addition of TRN, most NMR signals that are characteristic for glycine residues disappeared both in FUS454–526$_{WT}$ as well as in FUS454–526$_{P525L}$ (Figure 6C, left panels), demonstrating that the RGG motifs indeed bind to TRN. The NMR signal of the C-terminal tyrosine residue (Y526) disappeared upon addition of TRN in the WT protein,

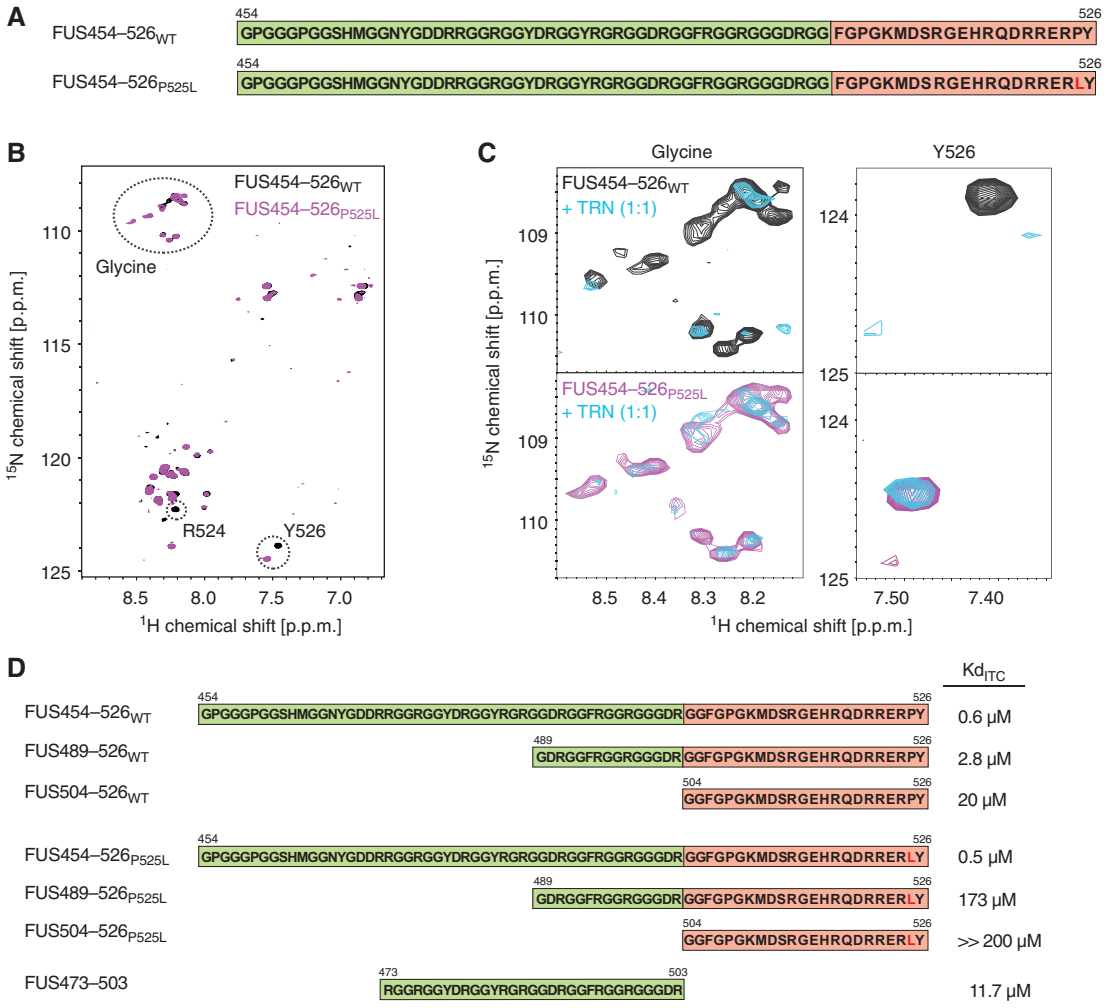

Figure 6 Both the RGG3 domain and the PY-NLS of FUS interact with TRN. (**A**) Schematic diagram of recombinant FUS proteins analysed by NMR spectroscopy. (**B**) Overlay of 2D $^{1}H,^{15}N$ HSQC NMR spectra recorded for FUS454–526$_{WT}$ (black) and FUS454–526$_{P525L}$ (magenta). Regions characteristic for glycine residues, position R524 and the C-terminal Y526 are encircled (dotted line). The distribution of NMR signals in regions characteristic for random coil proteins indicates that both proteins are intrinsically disordered in solution. (**C**) Overlay of selected regions (glycine and Y526) of 2D $^{1}H,^{15}N$ HSQC NMR spectra recorded for FUS454–526$_{WT}$ (black) and FUS454–526$_{P525L}$ (magenta) in isolation and in the presence of an equimolar stoichiometric equivalent of TRN (blue). NMR signals characteristic for glycine residues disappear upon addition of TRN, indicating binding of RGG repeats to TRN. The NMR signal of Y526 disappears upon addition of TRN in the WT protein, but is only slightly affected in the P525L mutant, indicating tight binding of TRN to the WT PY but not the mutant LY. (**D**) Schematic diagram of recombinant FUS proteins and synthetic FUS peptides analysed for TRN binding by ITC. Binding constants (Kd_{ITC}) are shown on the right. Both the PY-NLS and the N-terminal RGG repeats contribute to TRN binding. The RGG3 repeat domain can bind TRN in the absence of a C-terminal PY-NLS and can compensate for the lack of binding of the mutant C-terminus in the P525L mutant.

but was only slightly affected in FUS454–526$_{P525L}$ (Figure 6C, right panels), demonstrating binding of TRN to the C-terminal PY but not the mutant C-terminus. Thus, the P525L mutation disrupts binding of the C-terminal tyrosine to TRN, while the RGG3 repeat region interacts tightly with TRN in both WT and mutant FUS.

To quantitatively assess binding of the RGG3 repeat region to TRN, we studied the interaction of recombinant FUS454–526 or synthetic FUS peptides with TRN by isothermal titration calorimetry (ITC) (Figure 6D). This showed that both FUS454–526$_{WT}$ and FUS454–526$_{P525L}$ formed high-affinity complexes with TRN, with virtually identical dissociation constants below micromolar Kd (Supplementary Figure S1; Figure 6D). Thus, the binding affinity is unaffected by the C-terminal P525L mutation, suggesting that tight interaction between the unmethylated RGG3 domain and TRN can rescue weak binding of the C-terminus in the P525L mutant. Shorter FUS peptides lacking the N-terminal part of the RGG3 repeat region (FUS489–526$_{WT}$) or the entire RGG3 domain (FUS504–526$_{WT}$) bound to TRN with reduced affinities compared to FUS454–526$_{WT}$ (Figure 6D), confirming that the RGG3 repeats next to the PY-NLS stabilize the FUS–TRN interaction. The importance of the RGG3 repeat region for TRN binding became even more apparent in the context of the P525L mutation, where shortening or deletion of the RGG3 repeat region (FUS489–526$_{P525L}$ or FUS 504–526$_{P525L}$) severely impaired or completely prevented TRN binding (Figure 6D). Finally, we tested if the RGG3 domain alone was able to bind to TRN in the absence of a C-terminal PY-NLS. Indeed, a synthetic FUS peptide comprising the RGG3

repeat domain only (FUS473–503) bound to TRN with an affinity comparable to the WT PY-NLS ($FUS504–526_{WT}$) (Figure 6D). Taken together, our NMR and ITC analysis demonstrate that the unmethylated RGG3 domain of FUS binds tightly to TRN and that this interaction can even rescue weak binding of the mutant C-terminus in the ALS-associated P525L mutant.

Arginine methylation in the RGG3 domain of FUS impairs TRN binding

Based on our cellular assays, we speculated that arginine methylation in the RGG3 domain should impair TRN binding. To test this hypothesis, we performed *in vitro* pulldown assays with recombinant TRN and synthetic FUS peptides comprising the RGG3 domain either unmethylated or with asymmetrically dimethylated (me) arginine residues (FUS473–526 and meFUS473–503; see schematic diagram in Figure 7A). Biotinylated FUS peptides were immobilized on streptavidin beads and were incubated with varying amounts of recombinant His_6-tagged TRN or His_6–GST as a control. Consistent with our hypothesis, the unmethylated RGG3 peptide efficiently pulled down TRN, while TRN binding was undetectable for the methylated RGG3 peptide (Figure 7A). In line with these data, ITC and NMR showed TRN binding for the unmethylated FUS473–503 peptide, whereas no TRN binding could be observed for the methylated peptide (Figure 7A; Supplementary Figure S2A). Thus, arginine methylation in the RGG3 repeat domain of FUS strongly interferes with TRN binding.

We next investigated the effect of arginine methylation on TRN binding in the context of the C-terminal PY-NLS and thus performed *in vitro* pulldown assays with peptides comprising the WT or mutant PY-NLS preceded by four unmethylated or asymmetrically dimethylated RGG repeats ($FUS489–526_{WT}$, $meFUS489–526_{WT}$, $FUS489–526_{P525L}$ and $meFUS489–526_{P525L}$; see schematic diagrams in Figure 7B and C; these peptide were used since synthesis of longer peptides comprising the entire methylated RGG3 domain plus PY-NLS was not successful and *in vitro* methylation of the recombinant FUS454–526 proteins was very inefficient). We expected that arginine methylation would be especially detrimental for TRN binding of the P525L mutant, where binding of the C-terminal residues to TRN is strongly impaired (Figure 6C). Consistent with this hypothesis, arginine methylation strongly interfered with TRN binding of the mutant peptide in our pulldown assay (Figure 7B), and ITC and NMR showed weak TRN binding of the unmethylated $FUS489–526_{P525L}$ peptide and no binding of $meFUS489–526_{P525L}$ (Figure 7B; Supplementary Figure S2B). Interestingly, methylation also slightly impaired TRN binding of the WT peptide (Figure 7C), and ITC and NMR confirmed a reduced TRN binding affinity ($\sim$3-fold higher Kd) for $meFUS489–526_{WT}$ in comparison to $FUS489–526_{WT}$ (Figure 7C; Supplementary Figure S2C). Considering that the (me)$FUS489–526_{WT}$ peptides comprise only four RGG repeats and not the entire RGG3 domain, it seems likely that arginine methylation has a more dramatic effect on TRN binding in the presence of the entire RGG3 domain. Thus, arginine methylation in the RGG3 repeat domain not only impairs TRN binding of the FUS-P525L mutant, but also slightly modulates TRN binding of the WT protein.

Methylated FUS-P525L is recruited to stress granules upon cellular stress

Our finding that ALS-associated FUS mutants become nuclear upon inhibition of arginine methylation implies that mutant FUS must be methylated, since otherwise the mutant protein should be imported into the nucleus and it would be difficult to explain the correlation between nuclear transport defect and clinical phenotype (Dormann *et al*, 2010; Dormann and Haass, 2011). To test if FUS and ALS-associated FUS mutants are indeed methylated, we raised monoclonal antibodies specific to the methylated RGG3 domain (epitope meFUS473–503; Figure 8A). Two monoclonal antibodies (14H5 and 9G6) selectively recognized endogenous methylated FUS, since signals obtained by immunoblotting (Figure 8B) and immunofluorescence (Figure 8C) disappeared upon AdOx treatment or FUS knockdown. Methylated FUS was located exclusively in the nucleus both in HeLa cells (Figure 8C) and primary rat hippocampal neurons (Supplementary Figure S3C). In addition, cytosolic FUS mutants, such as FUS-P525L, were also recognized by the meFUS-specific antibodies (Figure 8D), which is consistent with our finding that inhibition of methylation restores nuclear localization of mutant FUS.

Stress granules have been suggested to be precursors of pathological FUS inclusions, since inclusions in ALS-FUS and FTLD-FUS patients are immunoreactive for stress granule marker proteins (Fujita *et al*, 2008; Dormann *et al*, 2010). We therefore used stress granules as a pathological surrogate for FUS inclusions and examined whether they contain methylated FUS-P525L. Consistent with our previous findings (Dormann *et al*, 2010; Bentmann *et al*, 2012), cytosolic FUS-P525L was recruited to stress granules in HeLa cells exposed to heat shock (Figure 8D). FUS-P525L-positive granules were not only co-stained with an antibody specific for the stress granule marker protein TIA-1, but also were co-labelled with a meFUS-specific antibody (Figure 8D). This demonstrates that methylated FUS-P525L is recruited to stress granules, the potential precursors of pathological FUS inclusions in ALS-FUS patients.

Inclusions in ALS-FUS contain methylated FUS, while inclusions in FTLD-FUS are hypomethylated

To investigate the methylation status of FUS in human brain, we analysed post mortem tissue from ALS-FUS, FTLD-FUS and healthy controls by immunohistochemistry and double-label immunofluorescence with the newly generated meFUS-specific antibodies. Like in cultured cells, the physiological staining pattern for meFUS was predominantly nuclear in controls and FUS-opathies (Supplementary Figure S3B and C). Consistent with our hypothesis that arginine methylation contributes to the pathological mislocalization of mutant FUS proteins, we revealed a very strong and consistent co-labelling of all FUS-positive cytoplasmic neuronal and glial inclusions with the meFUS antibody in all ALS-FUS cases investigated, including four different *FUS* mutations (Figure 9A). Thus, inclusions in ALS-FUS patients contain methylated FUS.

Next, we investigated the spectrum of FTLD-FUS, including atypical FTLD-U (aFTLD-U), neuronal intermediate filament inclusion body disease (NIFID) and basophilic inclusion body disease (BIBD). Surprisingly, FUS-positive neuronal and glial cytoplasmic inclusions as well as intranuclear inclusions in all

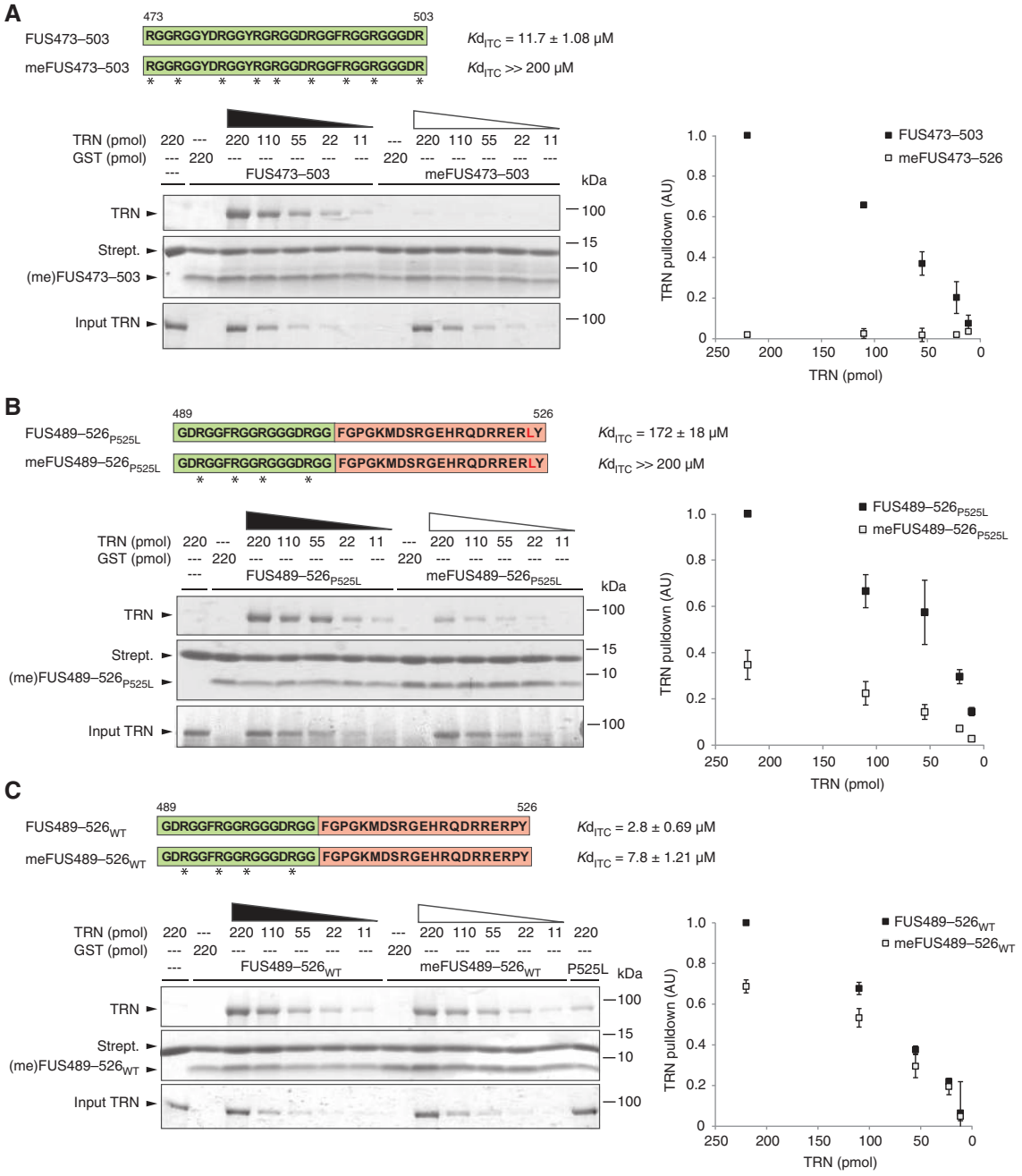

Figure 7 Arginine methylation in the RGG3 domain of FUS weakens TRN binding. *In vitro* pull-down assays with unmethylated and methylated (me) synthetic FUS peptides (see schematic diagrams for sequences, asterisks indicate asymmetric dimethyl groups) and recombinant TRN. Biotinylated peptides were immobilized on streptavidin beads and were incubated with the indicated amount of TRN–His_6 or His_6–GST as a control. Bound TRN was visualized by SDS–PAGE after Coomassie staining (upper panel). The middle panel shows the amount of streptavidin and peptide that was boiled off the streptavidin beads. Lower panel shows input of TRN. Plots on the right show a quantification of the TRN pulldown efficiency. The band with the highest intensity was set to 1.0 AU (arbitrary units) and relative intensities of other bands were calculated. Plots show means from two independent experiments, error bars indicate s.d. (**A**) The unmethylated RGG3 domain (FUS473–503) binds TRN in the absence of a PY-NLS and methylation abrogates this interaction. (**B**) Methylation strongly impairs TRN binding of the FUS489–526_{P525L} peptide. (**C**) Methylation slightly reduces TRN binding of the FUS489–526_{WT} peptide (~3-fold difference in Kd). Note that both FUS489–526_{WT} and meFUS489–526_{WT} bind TRN more tightly than FUS489–526_{P525L} (reference lane labelled 'P525L' on the right). Figure source data can be found with the Supplementary data.

FTLD-FUS subtypes were not labelled with the meFUS-specific antibody (Figure 9B), while a physiological nuclear staining was observed in all cases (Supplementary Figure S3B and C). Thus, in striking contrast to ALS-FUS, inclusions in FTLD-FUS appear to contain unmethylated FUS. This suggests hypomethylation of FUS (and potentially the other FET proteins) as a potential pathomechanism that might contribute to the co-deposition of FET proteins with TRN in FTLD-FUS.

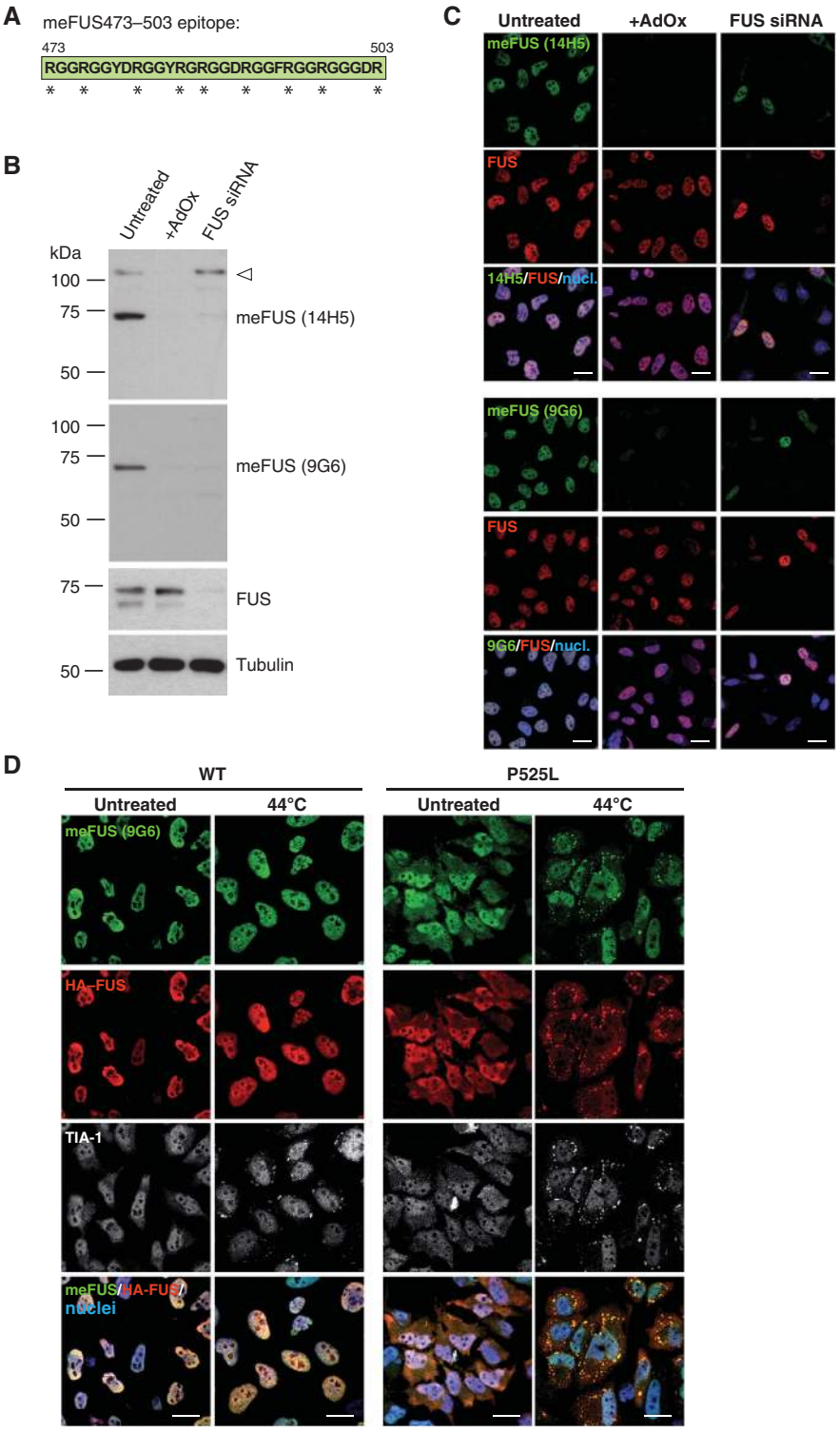

Figure 8 meFUS-specific monoclonal antibodies label ALS-associated FUS mutants in stress granules. (**A**) Schematic diagram of the peptide epitope (meFUS473–503) used for generation of meFUS-specific monoclonal antibodies. Asterisks denote asymmetric dimethyl groups. (**B**) Immunoblots show that monoclonal antibodies 14H5 and 9G6 are specific for methylated FUS, since staining is abrogated upon AdOx treatment and FUS knockdown. Open arrowhead indicates a non-specific methylated protein recognized by 14H5. Lower panels show FUS knockdown efficiency and Tubulin as a loading control. (**C**) Double-label immunocytochemistry of untransfected HeLa cells with meFUS-specific monoclonal antibodies 14H5 or 9G6 (green) and a polyclonal pan-FUS antibody (red). Both 14H5 and 9G6 specifically stain endogenous methylated FUS in the nuclei (blue). This staining is abrogated upon AdOx treatment and FUS knockdown. Scale bars: 20 μm. (**D**) HeLa cells stably expressing HA-tagged FUS-WT or HA–FUS-P525L were exposed to heat shock (44 °C) for 1 h prior to fixation or were kept at 37°C (untreated). Localization of methylated FUS was examined by confocal microscopy by co-labelling with a meFUS-specific antibody 9G6 (green), an HA-specific antibody (red), a TIA-1-specific antibody (white) and a nuclear counterstain (blue). Methylated FUS-P525L is recruited to TIA-1-positive stress granules after heat shock. Scale bars: 20 μm. Figure source data can be found with the Supplementary data.

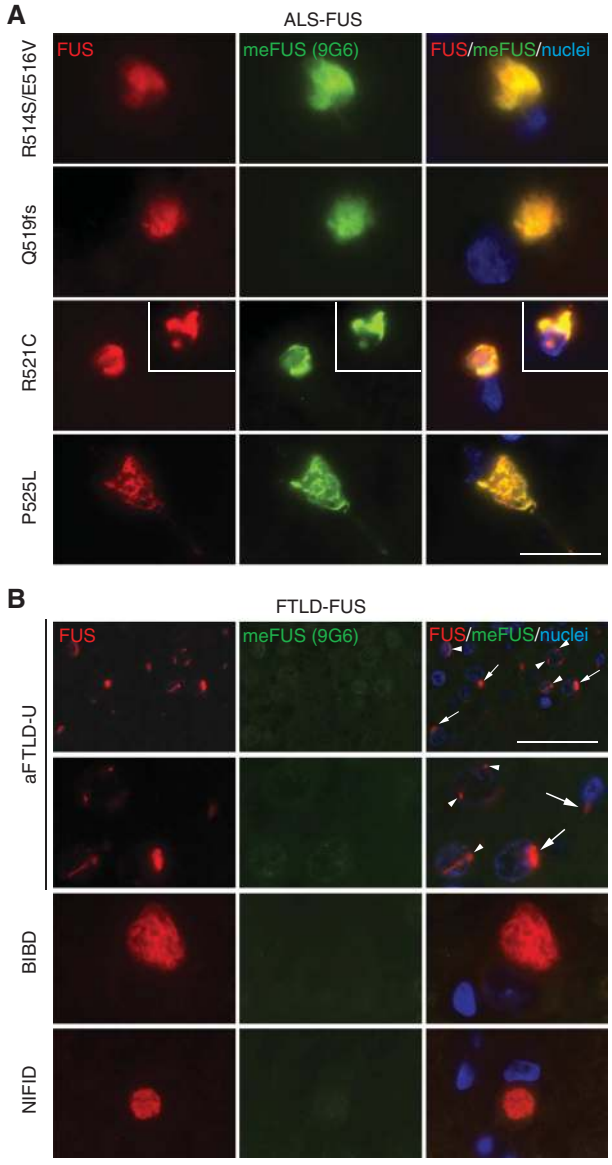

Figure 9 meFUS-specific monoclonal antibodies label FUS inclusions in ALS-FUS, but not in FTLD-FUS. (**A**) Double-label immunofluorescence of spinal cord sections from four ALS patients carrying different *FUS* mutations with a monoclonal antibody against meFUS (9G6, green), a polyclonal pan-FUS antibody (red) and nuclear counterstaining (blue). The characteristic FUS-positive neuronal cytoplasmic inclusions (rows 1–4) and glial inclusions (insert in row 3) in all ALS-FUS cases were intensely co-labelled by the meFUS-specific antibody. Scale bar: 20 μm. (**B**) Double-label immunofluorescence with a monoclonal antibody against meFUS (9G6, green), a polyclonal pan-FUS antibody (red) and nuclear counterstaining (blue) in the spectrum of FTLD-FUS, including aFTLD-U, BIBD and NIFID. In striking contrast to ALS-FUS, the meFUS-specific antibody did not label FUS-positive neuronal cytoplasmic inclusions (arrows in row 1 and 2) and neuronal intranuclear inclusions (arrowheads in row 1 and 2), as shown in dentate granule cells in aFTLD-U and the brainstem in BIBD and NIFID. Scale bar: 50 μm (row 1) or 20 μm (rows 2–4).

Discussion

By studying ALS-associated *FUS* mutations, we have uncovered a novel TRN-binding epitope, which is sensitive to arginine methylation. This broadens our perspective of TRN-cargo recognition, which classically has been thought to be determined by three modular, linear TRN-binding epitopes: (1) The PY of the C-terminal R/K/H/X_{2-5}PY motif, (2) the basic residue of the R/K/H/X_{2-5}PY motif and (3) an N-terminal hydrophobic or basic motif (Suel *et al*, 2008). Together, these three epitopes were described to constitute a signal of ~30 residues with intrinsic structural disorder and overall basic character (Lee *et al*, 2006; Suel *et al*, 2008). Based on these rules, Lee *et al* (2006) predicted a PY-NLS in the C-terminus of FUS and later on FUS residues 514–526 were shown to be necessary and sufficient for nuclear import in cultured cells and *in vivo* (Bosco *et al*, 2010; Dormann *et al*, 2010). Structural modelling of FUS residues 520–526 into the TRN-binding pocket showed that residues R522 and Y526 make strong H-bond interactions with TRN and that P525 allows a particular kinked geometry between P525 and Y526, leading to specific surface recognition of the two C-terminal residues by TRN (Dormann *et al*, 2010). Recently, the crystal structure of the FUS PY-NLS (residues 498–526) bound to TRN has been solved (Zhang and Chook, 2012). This revealed that the FUS PY-NLS consists of a C-terminal PY motif (1), an atypical arginine-rich polarized α-helix (2) and an N-terminal hydrophobic motif (3) (see schematic diagram in Figure 10A) and showed that residues mutated in ALS, for example, P525, make numerous contacts with TRN.

We studied longer recombinant FUS proteins (FUS454–526_{WT} and FUS454–526_{P525L}) in complex with TRN and surprisingly found that the RGG repeat domain preceding the PY-NLS interacts tightly with TRN and is even able to rescue weak binding of the C-terminus in the P525L mutant (Figure 6D). Moreover, the RGG3 domain can even bind to TRN independently of the PY-NLS, with an affinity comparable to the PY-NLS itself ($Kd_{ITC} = 11.7$ μM for FUS473–503 versus 20 μM for FUS504–526_{WT}). This defines the RGG repeat region adjacent to the PY-NLS of FUS as a novel TRN-binding motif and extends the classical PY-NLS consensus sequence with a fourth binding epitope (Figure 10A). Thus, at least for certain cargo proteins such as the FET proteins, the TRN-binding site can be much larger than previously anticipated. Interestingly, TRN also binds multiple proteins without a PY-NLS, such as ribosomal proteins, histones, c-Fos, HIV-Rev and others (Chook and Suel, 2011), suggesting that TRN can recognize different classes of NLSs. Our data suggest that unmethylated RGG repeats might be such a signal. Supporting this idea, the RGG domain of a putative TRN substrate, Cold-inducible RNA-binding protein (CIRP), is required for nuclear import of CIRP and arginine methylation causes cytoplasmic accumulation of CIRP (Aoki *et al*, 2002).

Nevertheless, our data have shown that epitope 1 and 2 of the (mutant) PY-NLS of FUS are still required for TRN binding, since a FUSΔ514–526 deletion mutant failed to be imported under conditions of methylation inhibition (Figure 4B). This suggests that the C-terminal TRN-binding epitopes might anchor the protein for further interaction of the RGG repeats with the negatively charged surface in the interior of TRN. In line with this hypothesis, addition of either the WT or mutant PY-NLS to the unmethylated RGG3 domain led to high-affinity interactions below micromolar Kd (Figure 6D). Taken together, our data suggest a novel model of FUS-TRN recognition (Figure 10B), where epitopes 1–3 of the PY-NLS anchor the FUS C-terminus to TRN and the adjacent RGG repeats stabilize the interaction, presumably

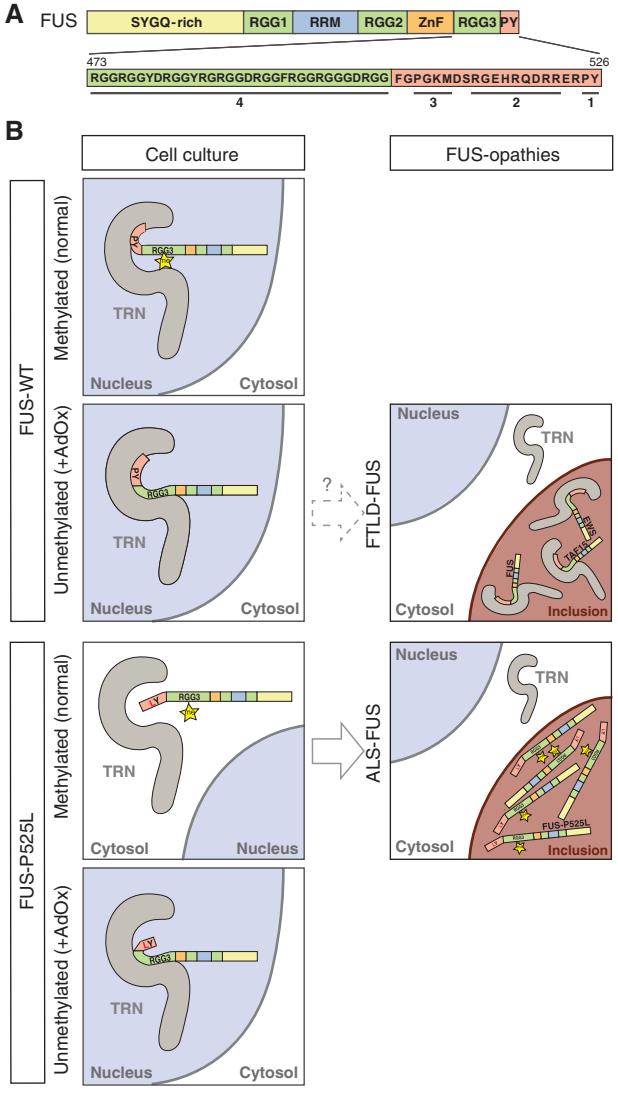

Figure 10 Model of the FUS–TRN interaction in cellular models and human FUSopathies. (**A**) Schematic diagram of FUS with sequences of the C-terminal PY-NLS (light red) and RGG3 domain (light green). Numbers indicate epitopes that contribute to TRN binding: 1 = C-terminal PY motif; 2 = central basic motif forming a polarized helix; 3 = N-terminal hydrophobic motif; 4 = RGG repeat region as a novel TRN-binding epitope. (**B**) Panels on the left show the interaction of methylated and unmethylated FUS-WT and FUS-P525L with TRN and the consequences for nuclear import in cultured cells. The PY-NLS of FUS is shown in light red and the RGG3 repeat region in light green. The yellow star denotes asymmetric dimethylation of the RGG3 domain. Panels on the right show the pathological situation in post mortem brains of FTLD-FUS and ALS-FUS patients. In FTLD-FUS, neuronal cytoplasmic inclusions contain all three FET proteins and TRN, but are not immunoreactive with meFUS-specific antibodies, suggesting that hypomethylation of the FET proteins and thus increased TRN binding may possibly be involved in the co-deposition of these proteins in FTLD-FUS. In contrast, ALS-FUS caused by *FUS* mutations is characterized by neuronal cytoplasmic inclusions that contain methylated FUS, but are negative for EWS, TAF15 and TRN. This suggests that the selective nuclear import defect of the FUS protein is caused by combination of a genetic defect (point mutation in TRN-binding epitopes 1–3) and post-translational modification (arginine methylation in TRN-binding epitope 4).

by interacting with the negatively charged surface in the interior of TRN. Methylation of the RGG repeats interferes strongly with TRN binding, probably due to changing hydrogen bonding and local hydrophobicity. In the methylated WT protein, the C-terminal epitopes nevertheless bind tightly enough to allow nuclear import, while in the methylated P525L mutant, weak binding of both epitopes 1 and 4 abrogates nuclear import, leading to cytoplasmic accumulation (Figure 10B).

It seems possible that other TRN substrates are modulated by arginine methylation in a similar fashion. Indeed, a recent study reported that arginine methylation of the nuclear poly(A) binding protein (PABPN1) weakens its interaction with TRN and that several nuclear proteins, including FUS, show increased TRN binding in PRMT1 knockout cells (Fronz *et al*, 2011). PABPN1 is methylated on key residues within the PY-NLS, such as the N-terminal basic cluster and the C-terminal RX_6PY motif (Smith *et al*, 1999; Lee *et al*, 2006), suggesting that in the case of PABPN1 arginine methylation within epitopes 2 and 3 of the PY-NLS might interfere with TRN binding. In contrast, FUS and the other FET proteins are methylated exclusively on arginine residues in epitope 4 (Belyanskaya *et al*, 2001; Rappsilber *et al*, 2003; Ong *et al*, 2004; Pahlich *et al*, 2005; Jobert *et al*, 2009) and our analysis has shown that arginine methylation within the RGG3 domain and not in other epitopes of the PY-NLS modulates TRN binding (Figure 5). Beyond the FET family proteins, several confirmed or predicted PY-NLS-containing proteins (Lee *et al*, 2006) contain methylated RGG motifs within the vicinity of the PY-NLS. Whether TRN-dependent nuclear import of these proteins is regulated by arginine methylation in a similar fashion remains to be shown.

Although ALS-FUS and FTLD-FUS have an overlapping clinical phenotype and neuropathology, the pathological inclusions in these two disorders were recently found to have a significantly different protein composition: Inclusions in ALS-FUS contain only the FUS protein, while inclusions in FTLD-FUS show a co-deposition of all FET proteins (FUS, EWS, and TAF15) and TRN (Brelstaff *et al*, 2011; Neumann *et al*, 2011, 2012; Davidson *et al*, 2012) (Figure 10B). Our study has revealed additional striking differences in the neuropathology of ALS-FUS and FTLD-FUS (Figure 9), further supporting the idea that the two disorders are caused by different pathomechanisms (Mackenzie and Neumann, 2012; Rademakers *et al*, 2012). In ALS-FUS, pathological inclusions contain methylated FUS, in line with the severe nuclear import defect observed for methylated FUS mutants in our cellular models (Figure 10B). Thus, arginine methylation seems to be required for the pathological mislocalization of ALS-associated FUS mutants and it is tempting to speculate that differences in arginine methylation might determine the age of disease onset, which can vary substantially between patients with the same point mutation (Kwiatkowski *et al*, 2009; Rademakers *et al*, 2010; Yan *et al*, 2010). Accordingly, we propose that ALS-FUS is a dominantly inherited human disease that might be modulated by a post-translational modification.

In contrast to ALS-FUS, which seems to be restricted to a dysfunction of FUS, FTLD-FUS appears to involve a more general defect in TRN-mediated nuclear import (Dormann and Haass, 2011; Mackenzie and Neumann, 2012; Rademakers *et al*, 2012). However, a general dysfunction or reduced expression of TRN seems unlikely, since none of 13 additional TRN cargo proteins investigated (e.g., heterogenous ribonucleoprotein A1, Sam68 and PABPN1) co-accumulate

with the FET proteins and TRN in FTLD-FUS (Neumann *et al*, 2012). Our data suggest that instead, defective arginine methylation of the FET proteins selectively alters their TRN-binding affinity (Figure 10B). Such hypomethylation of the FET proteins may lead to enhanced binding of the FET proteins to TRN and may hamper dissociation of FET–TRN transport complexes. Even though differences in TRN-binding affinity of methylated versus unmethylated FUS-WT may be small, it seems possible that over long periods of time, a slight increase in FET–TRN binding may lead to a co-deposition of FET proteins and TRN in cytoplasmic and nuclear inclusions in this late-onset neurodegenerative disease. It is also interesting to note that arginine methylation can affect protein aggregation, and in all reported cases hypomethylation favoured protein oligomerization/aggregation (Yu *et al*, 2004; Ostareck-Lederer *et al*, 2006; Perreault *et al*, 2007). Thus, hypomethylation might contribute to the pathological deposition of the FET proteins by affecting both their nuclear import and their aggregation behaviour.

What remains to be answered is how and why hypomethylation of the FET proteins might arise. The fact that PABPN1, which also binds to TRN with higher affinity in PRMT1 knockout cells (Fronz *et al*, 2011), is not co-deposited with FET proteins and TRN in FTLD-FUS (Neumann *et al*, 2012) argues against a general defect in arginine methylation and rather points to a selective hypomethylation of FET proteins. The question why hypomethylation of FET proteins might arise in FTLD-FUS brings up a related question, namely what is the physiological role of FET protein methylation in the first place? It can be speculated that arginine methylation of FET proteins reduces their affinity for TRN to a degree that allows for efficient dissociation of the import complex by RanGTP in the nucleus. Overly tight binding of hypomethylated FET proteins to TRN might hamper their dissociation from TRN in the nucleus, leading to re-export of FET–TRN complexes and ultimately to a reduction of FET proteins in the nucleus and co-deposition of FET and TRN in the cytoplasm (Figure 10B). Alternatively, it can be envisaged that arginine methylation of FET proteins is a fine-tuning mechanism to ensure that small amounts of newly synthesized FET proteins stay behind in the cytoplasm to fulfil important cytosolic functions. This would be in agreement with the findings that small amounts of cytosolic FUS are present in human and mouse brain (Neumann *et al*, 2009a; Aoki *et al*, 2012) and that FUS seems to play a role in mRNA transport to dendritic spines (Fujii and Takumi, 2005; Fujii *et al*, 2005; Liu-Yesucevitz *et al*, 2011). Additionally, FUS has been identified at focal adhesions and was shown to function in cell spreading (de Hoog *et al*, 2004). Finally, it cannot be excluded that arginine methylation regulates additional features of FET proteins, such as RNA binding or additional protein–protein interactions. The physiological role of arginine methylation of FET proteins and the mechanism behind a potential hypomethylation in FTLD-FUS certainly warrant further studies.

Materials and methods

Cell culture, transfection, inhibitor and stress treatment

Human cervical carcinoma cells (HeLa) were cultured and transfected as described previously (Dormann *et al*, 2010). HeLa cells stably expressing HA–FUS-WT or HA–FUS-P525L were generated by lentiviral transduction as described in Kuhn *et al* (2010), followed by selection with 0.5 μg/ml puromycin (Sigma). Hippocampal neurons were isolated from embryonic day 18 rats as described previously (Kaech and Banker, 2006). Neurons were plated at densities of 18 000 cells/cm^2 in 6 cm tissue culture dishes containing poly-L-lysine (1 mg/ml; Sigma-Aldrich)-coated glass coverslips and Neurobasal medium supplemented with 2% B27 and 0.5 mM glutamine (all from Invitrogen). On day *in vitro* (DIV) 7, cultured neurons were transfected with HA–FUS constructs using Lipofectamine 2000 (Invitrogen). YFP was co-transfected as a marker to visualize neuronal morphology. For all transient transfections, cells were analysed 24 h post-transfection. AdOx (Sigma) was dissolved in water and was used at a concentration of 20 μM (HeLa) or 10 μM (neurons) and was added to cells upon plating (HeLa) or DIV 7 (neurons) 9 h prior to transfection. Heat shock was performed by incubating cells for 1 h in a tissue culture incubator heated to 44°C.

Antibodies

A list of all commercially available antibodies used can be found in the Supplementary data. Rat monoclonal antibodies against an ovalbumin-conjugated meFUS473–503 peptide epitope were generated at the Institute of Molecular Immunology, Helmholtz Center Munich by standard procedures.

cDNA constructs and primers

All HA-tagged FUS, EWS and TAF15 constructs used for transient transfections were in pcDNA3.1/Hygro(−) (Invitrogen) and all GFP and GST–GFP constructs were in pEGFP–C1 (Clontech). Lentiviral HA–FUS constructs used for generation of stable HeLa cell lines were in pCDH-Ef1-MCS-IRES-Puro (System Biosciences). The cDNA encoding full-length human TRN with a C-terminal His_6-tag was in a pQE-60 vector (pQE-60-TRN–His_6) and was a generous gift of Dirk Görlich. The cDNA encoding His_6-tagged FUS454–526 (WT or P525L) was in a petM11-ZZ–His_6 vector. Details on cloning of mutant constructs can be found in the Supplementary data (Rydzanicz *et al*, 2005).

Recombinant proteins and synthetic peptides

Details on expression and purification of recombinant proteins can be found in the Supplementary data. Synthetic peptides (FUS473–503, meFUS473–503, FUS489–526$_{WT}$ and meFUS489–526$_{WT}$, FUS489–526$_{P525L}$, meFUS489–526$_{P525L}$, FUS504–526$_{WT}$ and FUS504–526$_{P525L}$) were synthesized and HPLC-purified by Peptide Specialty Laboratories GmbH, Heidelberg, Germany and were dissolved in TRN-binding buffer (20 mM sodium phosphate buffer, pH 6.8, 50 mM NaCl, 1 mM EDTA, 1 mM DTT).

Immunocytochemistry

Immunocytochemistry on HeLa cells was performed as described in Dormann *et al* (2010). Hippocampal neurons were fixed with 4% paraformaldehyde, quenched in 50 mM ammonium chloride for 10 min and permeabilized with 0.1% Triton X-100 for 3 min. After blocking with 2% fetal bovine serum (Invitrogen), 2% bovine serum albumin (Sigma-Aldrich) and 0.2% fish gelatin (Sigma-Aldrich) dissolved in phosphate-buffered saline, neurons were incubated with respective primary and secondary antibodies diluted in 10% blocking solution. DAPI (Invitrogen) was used as a nuclear counterstain.

Immunohistochemistry and immunofluorescence on human post mortem tissue

Immunohistochemistry conditions for meFUS antibodies were optimized using a tissue microarray that included formalin-fixed, paraffin-embedded biopsy material from a glioblastoma and a brain metastasis from a colon carcinoma as well as post mortem tissue from hippocampus and temporal cortex of three controls with no history of neurological disease. Studied FUS-opathy cases with robust pathology in selected neuroanatomical regions included aFTLD-U ($n=3$), BIBD ($n=1$), NIFID ($n=1$) and four ALS-FUS cases with three different missense and one truncation mutation, described in detail in previous studies (Neumann *et al*, 2011). Immunohistochemistry was performed on 5 μm thick paraffin sections using the NovoLinkTM Polymer Detection Kit and developed with 3,3′-diaminobenzidine. For double-label immunofluorescence, the secondary antibodies Alexa Fluor 594 and Alexa Fluor 488-conjugated anti-rabbit and anti-rat IgG (Invitrogen, 1:500) were used with Hoechst 33 342 (Sigma) for

nuclear counterstaining. Incubation with primary antibodies meFUS 9G6 (dilution 1:30) and anti-FUS HPA008784 (Sigma, 1:1000) was performed for 1 h at room temperature following microwave antigen retrieval.

Fluorescence image acquisition

Two or three-colour confocal images of HeLa cells were obtained with an inverted laser scanning confocal microscope (Zeiss LSM510) with a $\times 63/1.4$ oil immersion lens, using a pinhole diameter of 1 Airy unit. An image series along the z axis was taken and projected into a single image using the maximal projection tool of the LSM 510 software (Zeiss). Four-colour confocal images of HeLa cells were taken with an inverted laser scanning confocal microscope (Zeiss LSM710) with a $\times 40/1.4$ oil immersion lens. Using the Zen 2011 software (Zeiss), single confocal images were taken in the plane of the largest cytosolic area. For neurons, images were acquired with a wide-field fluorescence microscope (Axio Imager A2 inverted microscope and AxioVision software, both from Zeiss). For human post mortem tissue, immunofluorescence images were obtained by wide-field fluorescence microscopy (BX61 Olympus with digital camera F-view, Olympus). If necessary for printing, brightness and contrast were linearly enhanced using Adobe Photoshop's Level tool. Images and quantification shown are from one experiment, but are representative of at least three independent experiments.

Image quantification and statistics

Nuclear and cytosolic localization was quantified with the LSM 510 colocalization tool as follows: Total fluorescence intensities of the green channel were calculated from the mean fluorescence intensity (MFI) and the number of pixels. Pixels that were colocalized with the nuclear counterstain were considered 'nuclear' and pixels that did not overlap with the nuclear counterstain were considered 'cytosolic'. Typically 30–50 randomly selected cells (n) were analysed and mean values ± s.d. across n cells were calculated. Statistical analysis was carried out using the one-way ANOVA test with a Tukey post test. Images and quantification shown are from one experiment, but are representative of at least three independent experiments. For quantification of HA–FUS localization in neurons, 300 randomly selected cells per experiment ($n = 3$) were scored for cytoplasmic mislocalization of transfected HA–FUS constructs and the percentage of cells with mislocalized FUS ± s.d. were calculated. Statistical analysis was carried out using the unpaired two-tailed t-test.

siRNA-mediated knockdown

PRMT1 knockdown was achieved using two different PRMT1-specific siRNAs from Qiagen (Hs_HRMT1L2_7 and Hs_HRMT1L2_8). Negative control siRNA (Cat. No. 1022076, Qiagen) was used as a control. FUS knockdown was achieved using the ON-TARGET plus SMARTpool L-009497 from Dharmacon. Cells were reverse transfected using 20 pmol siRNA and 5 µl Lipofectamine 2000 (Invitrogen) per six-well. Medium was changed 4–6 h post-transfection and effect of knockdown was analysed 48 h (FUS knockdown) or 72 h (PRMT1 knockdown) post-transfection.

Cell lysates and immunoblotting

Total cell lysates were prepared in ice-cold RIPA buffer freshly supplemented with Complete Protease Inhibitor Cocktail (Roche). Lysates were sonicated (Bioruptor from Diagenode) and protein concentration was determined by BCA protein assay (Pierce). In all, $4\times$ SDS–PAGE sample buffer was added and samples were boiled for 5 min. Proteins were separated by SDS–PAGE, transferred onto a PVDF membrane (Immobilon-P, Millipore) and analysed by immunoblotting using the indicated antibodies. Bound antibodies were detected with the chemiluminescence detection reagents ECL or ECL prime (both from Amersham) or Immobilon (Millipore).

In vitro pulldown assay

N-terminally biotinylated peptides were immobilized on streptavidin sepharose beads (GE Healthcare, 440 pmol peptide/5 µl beads) and were blocked in wash buffer (20 mM sodium phosphate buffer pH 7.4, 150 mM KCl, 0.5 mM EDTA, 5 mM $MgCl_2$, 10% glycerol, 1 mM DTT) supplemented with 0.5 mg/ml BSA. In all, 5 µl peptide-loaded beads were incubated with the indicated amounts of recombinant TRN–His_6 or His_6–GST in 500 µl of the same buffer for 1–3 h at 4°C. Beads were washed three times in wash buffer and boiled for 3 min in $2\times$ SDS–PAGE sample buffer. Eluted proteins were separated by SDS–PAGE (10–20%) and visualized by staining with GelCode Blue Stain Reagent (Thermo Scientific). Band intensities were quantified using the MultiGaugeV3.0 programme. After background subtraction, the band with the highest pixel number was set to 1.0 AU (arbitrary units).

Isothermal titration calorimetry

Binding affinities of FUS peptides and recombinant proteins to TRN were determined using ITC on a VP-ITC Microcal calorimeter (Microcal, Northhampton, USA) at 25°C or 10°C (FUS473–503; due to entropy–enthalpy compensation at 25°C) with 35 rounds of 12 µl injections. All proteins/peptides were dialyzed or dissolved in TRN-binding buffer. The ITC data were analysed with the program MicroCal Origin software version 7.0 and single site binding model.

NMR experiments

Samples for NMR measurements contained 0.008–0.012 mM protein in TRN-binding buffer with 10% ^2H_2O added for the lock signal. For the TRN bound measurements, ^{15}N isotope labelled FUS454–526_{WT} and FUS454–526_{P525L} were titrated with increasing amounts of unlabelled TRN to stoichiometric ratios (FUS:TRN) of 1:0.1, 1:0.3, 1:0.5, 1:0.7, 1:1 and 1:2.6. Spectral changes were monitored by 1D ^1H and 2D $^1H,^{15}N$ HSQC spectra in each step of the titration. For the FUS peptide bound measurements, unlabelled TRN was titrated with increasing amounts of FUS peptides (FUS473–503, meFUS473–503, FUS489–526_{P525L}, meFUS489–$526_{P525L,}$ FUS489–526_{WT}, meFUS489–526_{WT}) to stoichiometric ratios (TRN:FUS) of 1:0.25, 1:0.5, 1:1. Spectral changes were monitored by 1D ^1H spectra in each step of the titration. Details on NMR spectra recording and processing can be found in the Supplementary data.

Supplementary data

Supplementary data are available at *The EMBO Journal* Online (http://www.embojournal.org).

Acknowledgements

We thank Dirk Görlich for generous gifts of plasmids, Sven Lammich for providing human brain cDNA, Julia Strathmann for help with statistics, Harald Steiner for reagents, Sebastian Hogl and Stefan Lichtenthaler for purified His_6–GST. We thank Rita Kemkes, Brigitte Nuscher, Andrea Seibel and Stephanie Kunath for technical assistance. We are grateful to Peter Macheroux and Silvia Wallner for access to the ITC instrument and technical assistance and to Maria Funke and Konstanze Winklhofer for lentiviral vectors and virus production protocols. We thank Anja Capell, Dieter Edbauer, Bettina Schmid and Harald Steiner for critically reading the manuscript and helpful discussion. This work was supported by the Sonderforschungsbereich Molecular Mechanisms of Neurodegeneration (SFB 596, CH and EK), the Competence Network for Neurodegenerative Diseases (KNDD) of the Bundesministerium für Bildung und Forschung (BMBF, CH and MN) and the Swiss National Science Foundation (31003A-132864, MN). DD was supported by the Robert Bosch Foundation. TM was supported by the Austrian Academy of Sciences (APART-fellowship), the Bavarian Ministry of Sciences, Research and the Arts in the framework of the Bavarian Molecular Biosystems Research Network and the German Research Foundation (DFG, Emmy Noether program MA 5703/1-1). EB was supported by the Elite Network of Bavaria. OA was supported by the NIHR Oxford Biomedical Research Centre. IM was funded by the Canadian Institutes of Health Research Grants 179009 and 74580 and the Pacific Alzheimer's Research Foundation centre Grant C06-01. CH was supported by a 'Forschungsprofessur' of the Ludwig-Maximilians University. We thank the Hans and Ilse Breuer Foundation for the Confocal Microscope.

Author contributions: DD cloned most constructs, performed and analysed most cell culture experiments, purified recombinant FUS proteins, performed *in vitro* pulldown assays and characterized meFUS-specific antibodies. TM purified recombinant TRN and performed and analysed NMR and ITC experiments. CV and MN characterized meFUS-specific antibodies on human tissue and

performed the immunohistochemistry and immunofluorescence analysis on human brain tissue. EB generated stable HeLa cell lines, cloned EWS and TAF15 constructs and analysed FET protein localization upon AdOx treatment. ST performed experiments with primary neuronal cultures. CA provided technical assistance and screened monoclonal antibodies. EK generated meFUS-specific monoclonal antibodies. OA and IM provided human post mortem material from FTLD-FUS and ALS-FUS cases and were involved in the interpretation of data. DD and CH designed and supervised the project and DD wrote the manuscript with input from all authors. CH applied for and obtained a grant from an anonymous foundation for this project.

Conflict of interest

The authors declare that they have no conflict of interest.

References

Aoki K, Ishii Y, Matsumoto K, Tsujimoto M (2002) Methylation of Xenopus CIRP2 regulates its arginine- and glycine-rich region-mediated nucleocytoplasmic distribution. *Nucleic Acids Res* **30:** 5182–5192

Aoki N, Higashi S, Kawakami I, Kobayashi Z, Hosokawa M, Katsuse O, Togo T, Hirayasu Y, Akiyama H (2012) Localization of fused in sarcoma (FUS) protein to the post-synaptic density in the brain. *Acta Neuropathol* **124:** 383–394

Araya N, Hiraga H, Kako K, Arao Y, Kato S, Fukamizu A (2005) Transcriptional down-regulation through nuclear exclusion of EWS methylated by PRMT1. *Biochem Biophys Res Commun* **329:** 653–660

Bartel RL, Borchardt RT (1984) Effects of adenosine dialdehyde on S-adenosylhomocysteine hydrolase and S-adenosylmethionine-dependent transmethylations in mouse L929 cells. *Mol Pharmacol* **25:** 418–424

Baumer D, Hilton D, Paine SM, Turner MR, Lowe J, Talbot K, Ansorge O (2010) Juvenile ALS with basophilic inclusions is a FUS proteinopathy with FUS mutations. *Neurology* **75:** 611–618

Bedford MT, Clarke SG (2009) Protein arginine methylation in mammals: who, what, and why. *Mol Cell* **33:** 1–13

Belyanskaya LL, Gehrig PM, Gehring H (2001) Exposure on cell surface and extensive arginine methylation of ewing sarcoma (EWS) protein. *J Biol Chem* **276:** 18681–18687

Bentmann E, Neumann M, Tahirovic S, Rodde R, Dormann D, Haass C (2012) Requirements for stress granule recruitment of fused in sarcoma (FUS) and TAR DNA-binding protein of 43 kDa (TDP-43). *J Biol Chem* **287:** 23079–23094

Blair IP, Williams KL, Warraich ST, Durnall JC, Thoeng AD, Manavis J, Blumbergs PC, Vucic S, Kiernan MC, Nicholson GA (2010) FUS mutations in amyotrophic lateral sclerosis: clinical, pathological, neurophysiological and genetic analysis. *J Neurol Neurosurg Psychiatry* **81:** 639–645

Bosco DA, Lemay N, Ko HK, Zhou H, Burke C, Kwiatkowski Jr TJ, Sapp P, McKenna-Yasek D, Brown Jr. RH, Hayward LJ (2010) Mutant FUS proteins that cause amyotrophic lateral sclerosis incorporate into stress granules. *Hum Mol Genet* **19:** 4160–4175

Brelstaff J, Lashley T, Holton JL, Lees AJ, Rossor MN, Bandopadhyay R, Revesz T (2011) Transportin1: a marker of FTLD-FUS. *Acta Neuropathol* **122:** 591–600

Butler JS, Zurita-Lopez CI, Clarke SG, Bedford MT, Dent SY (2011) Protein-arginine methyltransferase 1 (PRMT1) methylates Ash2L, a shared component of mammalian histone H3K4 methyltransferase complexes. *J Biol Chem* **286:** 12234–12244

Cansizoglu AE, Lee BJ, Zhang ZC, Fontoura BM, Chook YM (2007) Structure-based design of a pathway-specific nuclear import inhibitor. *Nat Struct Mol Biol* **14:** 452–454

Chen DH, Wu KT, Hung CJ, Hsieh M, Li C (2004) Effects of adenosine dialdehyde treatment on in vitro and in vivo stable protein methylation in HeLa cells. *J Biochem* **136:** 371–376

Chio A, Restagno G, Brunetti M, Ossola I, Calvo A, Mora G, Sabatelli M, Monsurro MR, Battistini S, Mandrioli J, Salvi F, Spataro R, Schymick J, Traynor BJ, La Bella V (2009) Two Italian kindreds with familial amyotrophic lateral sclerosis due to FUS mutation. *Neurobiol Aging* **30:** 1272–1275

Chook YM, Suel KE (2011) Nuclear import by karyopherin-betas: recognition and inhibition. *Biochim Biophys Acta* **1813:** 1593–1606

Da Cruz S, Cleveland DW (2011) Understanding the role of TDP-43 and FUS/TLS in ALS and beyond. *Curr Opin Neurobiol* **21:** 904–919

Davidson YS, Robinson AC, Hu Q, Mishra M, Baborie A, Jaros E, Perry RH, Cairns NJ, Richardson A, Gerhard A, Neary D, Snowden JS, Bigio EH, Mann DM (2012) Nuclear carrier and RNA binding proteins in frontotemporal lobar degeneration associated with fused in sarcoma (FUS) pathological changes. *Neuropathol Appl Neurobiol* doi:10.1111/j.1365-2990.2012.01274.x

de Hoog CL, Foster LJ, Mann M (2004) RNA and RNA binding proteins participate in early stages of cell spreading through spreading initiation centers. *Cell* **117:** 649–662

DeJesus-Hernandez M, Kocerha J, Finch N, Crook R, Baker M, Desaro P, Johnston A, Rutherford N, Wojtas A, Kennelly K, Wszolek ZK, Graff-Radford N, Boylan K, Rademakers R (2010) De novo truncating FUS gene mutation as a cause of sporadic amyotrophic lateral sclerosis. *Hum Mutat* **31:** E1377–E1389

Dormann D, Haass C (2011) TDP-43 and FUS: a nuclear affair. *Trends Neurosci* **34:** 339–348

Dormann D, Rodde R, Edbauer D, Bentmann E, Fischer I, Hruscha A, Than ME, Mackenzie IR, Capell A, Schmid B, Neumann M, Haass C (2010) ALS-associated fused in sarcoma (FUS) mutations disrupt Transportin-mediated nuclear import. *EMBO J* **29:** 2841–2857

Du K, Arai S, Kawamura T, Matsushita A, Kurokawa R (2011) TLS and PRMT1 synergistically coactivate transcription at the survivin promoter through TLS arginine methylation. *Biochem Biophys Res Commun* **404:** 991–996

Fronz K, Guttinger S, Burkert K, Kuhn U, Stohr N, Schierhorn A, Wahle E (2011) Arginine methylation of the nuclear poly(a) binding protein weakens the interaction with its nuclear import receptor, transportin. *J Biol Chem* **286:** 32986–32994

Fujii R, Okabe S, Urushido T, Inoue K, Yoshimura A, Tachibana T, Nishikawa T, Hicks GG, Takumi T (2005) The RNA binding protein TLS is translocated to dendritic spines by mGluR5 activation and regulates spine morphology. *Curr Biol* **15:** 587–593

Fujii R, Takumi T (2005) TLS facilitates transport of mRNA encoding an actin-stabilizing protein to dendritic spines. *J Cell Sci* **118:** 5755–5765

Fujita K, Ito H, Nakano S, Kinoshita Y, Wate R, Kusaka H (2008) Immunohistochemical identification of messenger RNA-related proteins in basophilic inclusions of adult-onset atypical motor neuron disease. *Acta Neuropathol* **116:** 439–445

Gal J, Zhang J, Kwinter DM, Zhai J, Jia H, Jia J, Zhu H (2011) Nuclear localization sequence of FUS and induction of stress granules by ALS mutants. *Neurobiol Aging* **32:** e2327–e2340

Groen EJ, van Es MA, van Vught PW, Spliet WG, van Engelen-Lee J, de Visser M, Wokke JH, Schelhaas HJ, Ophoff RA, Fumoto K, Pasterkamp RJ, Dooijes D, Cuppen E, Veldink JH, van den Berg LH (2010) FUS mutations in familial amyotrophic lateral sclerosis in the Netherlands. *Arch Neurol* **67:** 224–230

Hewitt C, Kirby J, Highley JR, Hartley JA, Hibberd R, Hollinger HC, Williams TL, Ince PG, McDermott CJ, Shaw PJ (2010) Novel FUS/TLS mutations and pathology in familial and sporadic amyotrophic lateral sclerosis. *Arch Neurol* **67:** 455–461

Hung CJ, Lee YJ, Chen DH, Li C (2009) Proteomic analysis of methylarginine-containing proteins in HeLa cells by two-dimensional gel electrophoresis and immunoblotting with a methylarginine-specific antibody. *Protein J* **28:** 139–147

Ito D, Seki M, Tsunoda Y, Uchiyama H, Suzuki N (2011) Nuclear transport impairment of amyotrophic lateral sclerosis-linked mutations in FUS/TLS. *Ann Neurol* **69:** 152–162

Jobert L, Argentini M, Tora L (2009) PRMT1 mediated methylation of TAF15 is required for its positive gene regulatory function. *Exp Cell Res* **315:** 1273–1286

Kaech S, Banker G (2006) Culturing hippocampal neurons. *Nat Protoc* **1:** 2406–2415

Kiernan MC, Vucic S, Cheah BC, Turner MR, Eisen A, Hardiman O, Burrell JR, Zoing MC (2011) Amyotrophic lateral sclerosis. *Lancet* **377:** 942–955

Kino Y, Washizu C, Aquilanti E, Okuno M, Kurosawa M, Yamada M, Doi H, Nukina N (2010) Intracellular localization and splicing regulation of FUS/TLS are variably affected by amyotrophic lateral sclerosis-linked mutations. *Nucleic Acids Res* **39:** 2781–2798

Kosugi S, Hasebe M, Entani T, Takayama S, Tomita M, Yanagawa H (2008) Design of peptide inhibitors for the importin alpha/beta nuclear import pathway by activity-based profiling. *Chem Biol* **15:** 940–949

Kuhn PH, Wang H, Dislich B, Colombo A, Zeitschel U, Ellwart JW, Kremmer E, Rossner S, Lichtenthaler SF (2010) ADAM10 is the physiologically relevant, constitutive alpha-secretase of the amyloid precursor protein in primary neurons. *EMBO J* **29:** 3020–3032

Kwiatkowski Jr TJ, Bosco DA, Leclerc AL, Tamrazian E, Vanderburg CR, Russ C, Davis A, Gilchrist J, Kasarskis EJ, Munsat T, Valdmanis P, Rouleau GA, Hosler BA, Cortelli P, de Jong PJ, Yoshinaga Y, Haines JL, Pericak-Vance MA, Yan J, Ticozzi N *et al* (2009) Mutations in the FUS/TLS gene on chromosome 16 cause familial amyotrophic lateral sclerosis. *Science* **323:** 1205–1208

Lagier-Tourenne C, Polymenidou M, Cleveland DW (2010) TDP-43 and FUS/TLS: emerging roles in RNA processing and neurodegeneration. *Hum Mol Genet* **19:** R46–R64

Lee BJ, Cansizoglu AE, Suel KE, Louis TH, Zhang Z, Chook YM (2006) Rules for nuclear localization sequence recognition by karyopherin beta 2. *Cell* **126:** 543–558

Lee J, Bedford MT (2002) PABP1 identified as an arginine methyltransferase substrate using high-density protein arrays. *EMBO Rep* **3:** 268–273

Liteplo RG, Kerbel RS (1986) Periodate-oxidized adenosine induction of murine thymidine kinase: role of DNA methylation in the generation of tumor cell heterogeneity. *Cancer Res* **46:** 577–582

Liu-Yesucevitz L, Bassell GJ, Gitler AD, Hart AC, Klann E, Richter JD, Warren ST, Wolozin B (2011) Local RNA translation at the synapse and in disease. *J Neurosci* **31:** 16086–16093

Lomen-Hoerth C, Anderson T, Miller B (2002) The overlap of amyotrophic lateral sclerosis and frontotemporal dementia. *Neurology* **59:** 1077–1079

Mackenzie IR, Ansorge O, Strong M, Bilbao J, Zinman L, Ang LC, Baker M, Stewart H, Eisen A, Rademakers R, Neumann M (2011) Pathological heterogeneity in amyotrophic lateral sclerosis with FUS mutations: two distinct patterns correlating with disease severity and mutation. *Acta Neuropathol* **122:** 87–98

Mackenzie IR, Neumann M (2012) FET proteins in frontotemporal dementia and amyotrophic lateral sclerosis. *Brain Res* **1462:** 40–43

Mackenzie IR, Neumann M, Bigio EH, Cairns NJ, Alafuzoff I, Kril J, Kovacs GG, Ghetti B, Halliday G, Holm IE, Ince PG, Kamphorst W, Revesz T, Rozemuller AJ, Kumar-Singh S, Akiyama H, Baborie A, Spina S, Dickson DW, Trojanowski JQ *et al* (2010a) Nomenclature and nosology for neuropathologic subtypes of frontotemporal lobar degeneration: an update. *Acta Neuropathol* **119:** 1–4

Mackenzie IR, Rademakers R, Neumann M (2010b) TDP-43 and FUS in amyotrophic lateral sclerosis and frontotemporal dementia. *Lancet Neurol* **9:** 995–1007

Murphy JM, Henry RG, Langmore S, Kramer JH, Miller BL, Lomen-Hoerth C (2007) Continuum of frontal lobe impairment in amyotrophic lateral sclerosis. *Arch Neurol* **64:** 530–534

Neumann M, Bentmann E, Dormann D, Jawaid A, DeJesus-Hernandez M, Ansorge O, Roeber S, Kretzschmar HA, Munoz DG, Kusaka H, Yokota O, Ang LC, Bilbao J, Rademakers R, Haass C, Mackenzie IR (2011) FET proteins TAF15 and EWS are selective markers that distinguish FTLD with FUS pathology from amyotrophic lateral sclerosis with FUS mutations. *Brain* **134:** 2595–2609

Neumann M, Rademakers R, Roeber S, Baker M, Kretzschmar HA, Mackenzie IR (2009a) A new subtype of frontotemporal lobar degeneration with FUS pathology. *Brain* **132:** 2922–2931

Neumann M, Roeber S, Kretzschmar HA, Rademakers R, Baker M, Mackenzie IR (2009b) Abundant FUS-immunoreactive pathology in neuronal intermediate filament inclusion disease. *Acta Neuropathol* **118:** 605–616

Neumann M, Valori CF, Ansorge O, Kretzschmar HA, Munoz DG, Kusaka H, Yokota O, Ishihara K, Ang LC, Bilbao JM, Mackenzie IR (2012) Transportin 1 accumulates specifically with FET proteins but no other transportin cargos in FTLD-FUS and is absent in FUS inclusions in ALS with FUS mutations. *Acta Neuropathol* doi:10.1007/s00401-012-1020-6

Ong SE, Mittler G, Mann M (2004) Identifying and quantifying in vivo methylation sites by heavy methyl SILAC. *Nat Methods* **1:** 119–126

Ostareck-Lederer A, Ostareck DH, Rucknagel KP, Schierhorn A, Moritz B, Huttelmaier S, Flach N, Handoko L, Wahle E (2006) Asymmetric arginine dimethylation of heterogeneous nuclear ribonucleoprotein K by protein-arginine methyltransferase 1 inhibits its interaction with c-Src. *J Biol Chem* **281:** 11115–11125

Pahlich S, Bschir K, Chiavi C, Belyanskaya L, Gehring H (2005) Different methylation characteristics of protein arginine methyltransferase 1 and 3 toward the Ewing Sarcoma protein and a peptide. *Proteins* **61:** 164–175

Pahlich S, Zakaryan RP, Gehring H (2006) Protein arginine methylation: Cellular functions and methods of analysis. *Biochim Biophys Acta* **1764:** 1890–1903

Pawlak MR, Scherer CA, Chen J, Roshon MJ, Ruley HE (2000) Arginine N-methyltransferase 1 is required for early postimplantation mouse development, but cells deficient in the enzyme are viable. *Mol Cell Biol* **20:** 4859–4869

Perreault A, Lemieux C, Bachand F (2007) Regulation of the nuclear poly(A)-binding protein by arginine methylation in fission yeast. *J Biol Chem* **282:** 7552–7562

Rademakers R, Neumann M, Mackenzie IR (2012) Advances in understanding the molecular basis of frontotemporal dementia. *Nat Rev Neurol* **8:** 423–434

Rademakers R, Stewart H, Dejesus-Hernandez M, Krieger C, Graff-Radford N, Fabros M, Briemberg H, Cashman N, Eisen A, Mackenzie IR (2010) Fus gene mutations in familial and sporadic amyotrophic lateral sclerosis. *Muscle Nerve* **42:** 170–176

Rappsilber J, Friesen WJ, Paushkin S, Dreyfuss G, Mann M (2003) Detection of arginine dimethylated peptides by parallel precursor ion scanning mass spectrometry in positive ion mode. *Anal Chem* **75:** 3107–3114

Rydzanicz R, Zhao XS, Johnson PE (2005) Assembly PCR oligo maker: a tool for designing oligodeoxynucleotides for constructing long DNA molecules for RNA production. *Nucleic Acids Res* **33:** W521–W525

Smith JJ, Rucknagel KP, Schierhorn A, Tang J, Nemeth A, Linder M, Herschman HR, Wahle E (1999) Unusual sites of arginine methylation in Poly(A)-binding protein II and in vitro methylation by protein arginine methyltransferases PRMT1 and PRMT3. *J Biol Chem* **274:** 13229–13234

Snowden JS, Hu Q, Rollinson S, Halliwell N, Robinson A, Davidson YS, Momeni P, Baborie A, Griffiths TD, Jaros E, Perry RH, Richardson A, Pickering-Brown SM, Neary D, Mann DM (2011) The most common type of FTLD-FUS (aFTLD-U) is associated with a distinct clinical form of frontotemporal dementia but is not related to mutations in the FUS gene. *Acta Neuropathol* **122:** 99–110

Suel KE, Gu H, Chook YM (2008) Modular organization and combinatorial energetics of proline-tyrosine nuclear localization signals. *PLoS Biol* **6:** e137

Tang J, Frankel A, Cook RJ, Kim S, Paik WK, Williams KR, Clarke S, Herschman HR (2000) PRMT1 is the predominant type I protein arginine methyltransferase in mammalian cells. *J Biol Chem* **275:** 7723–7730

Terry LJ, Shows EB, Wente SR (2007) Crossing the nuclear envelope: hierarchical regulation of nucleocytoplasmic transport. *Science* **318:** 1412–1416

Tradewell ML, Yu Z, Tibshirani M, Boulanger MC, Durham HD, Richard S (2012) Arginine methylation by PRMT1 regulates nuclear-cytoplasmic localization and toxicity of FUS/TLS harbouring ALS-linked mutations. *Hum Mol Genet* **21:** 136–149

Urwin H, Josephs KA, Rohrer JD, Mackenzie IR, Neumann M, Authier A, Seelaar H, Van Swieten JC, Brown JM, Johannsen P, Nielsen JE, Holm IE, Dickson DW, Rademakers R, Graff-Radford NR, Parisi JE, Petersen RC, Hatanpaa KJ, White 3rd CL, Weiner MF *et al* (2010) FUS pathology defines the majority of tau- and TDP-43-negative frontotemporal lobar degeneration. *Acta Neuropathol* **120:** 33–41

Vance C, Rogelj B, Hortobagyi T, De Vos KJ, Nishimura AL, Sreedharan J, Hu X, Smith B, Ruddy D, Wright P, Ganesalingam J, Williams KL, Tripathi V, Al-Saraj S, Al-Chalabi A, Leigh PN, Blair IP, Nicholson G, de Belleroche J, Gallo JM *et al* (2009) Mutations in FUS, an RNA processing protein, cause familial amyotrophic lateral sclerosis type 6. *Science* **323:** 1208–1211

Waibel S, Neumann M, Rabe M, Meyer T, Ludolph AC (2010) Novel missense and truncating mutations in FUS/TLS in familial ALS. *Neurology* **75:** 815–817

Yan J, Deng HX, Siddique N, Fecto F, Chen W, Yang Y, Liu E, Donkervoort S, Zheng JG, Shi Y, Ahmeti KB, Brooks B, Engel WK, Siddique T (2010) Frameshift and novel mutations in FUS in familial amyotrophic lateral sclerosis and ALS/dementia. *Neurology* **75:** 807–814

Yu MC, Bachand F, McBride AE, Komili S, Casolari JM, Silver PA (2004) Arginine methyltransferase affects interactions and recruitment of mRNA processing and export factors. *Genes Dev* **18:** 2024–2035

Zhang ZC, Chook YM (2012) Structural and energetic basis of ALS-causing mutations in the atypical proline-tyrosine nuclear localization signal of the Fused in Sarcoma protein (FUS). *Proc Natl Acad Sci USA* **109:** 12017–12021